Metabollic Engineering of Saccharomyces Cereviae a,omi acid metabolism for production of products of industrial interest

Chen, Xiao

Publication date:
2011

Document Version
Publisher's PDF, also known as Version of record

Metabolic engineering of *Saccharomyces cerevisiae* amino acid metabolism for production of chemicals of industrial interest

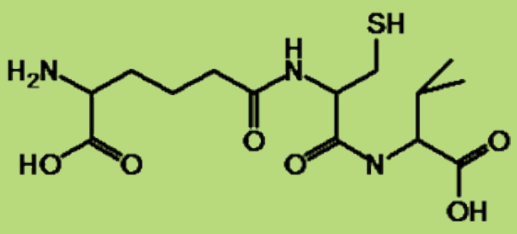

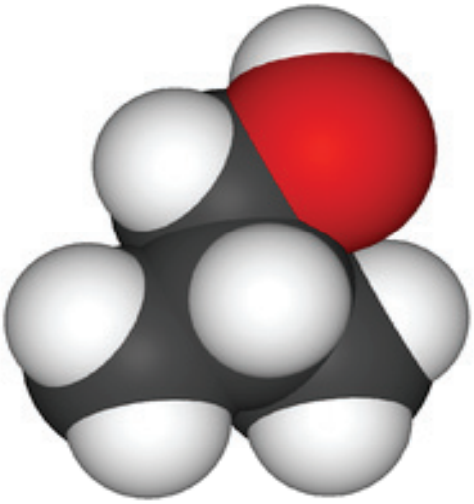

Xiao Chen
Ph.D. Thesis
June 2011

Center for Microbial Biotechnology
Department of Systems Biology

Metabolic engineering of *Saccharomyces cerevisiae* amino acid metabolism for production of chemicals of industrial interest

Ph.D. thesis

Xiao Chen

Center for Microbial Biotechnology

Department of Systems Biology

Technical University of Denmark

2011

Metabolic engineering af aminosyrestofskiftet hos *Saccharomyces cerevisiae* for produktion af kemikalier af industriel interesse

Ph.D.-afhandling

Xiao Chen

Center for Mikrobiel Bioteknologi

Institut for Systembiologi

Danmarks Tekniske Universitet

2011

Address: Center for Microbial Biotechnology
Department of Systems Biology
Technical University of Denmark
Building 223
DK-2800 Kgs. Lyngby
Denmark
Phone: +45 4525 2693
Fax: +45 4588 4148
Web: www.cmb.dtu.dk

Print: J&R Frydenberg A/S
København
September 2011

ISBN: 978-87-9149499-4

This Ph.D. project is funded by the Technical University of Denmark. It started in December of 2006 with Professor Jens Nielsen as main supervisor and PostDoc Verena Siewers as cosupervisor. In January of 2009 the project was reformulated. From January of 2009 to March of 2011, Professor Morten C. Kielland-Brandt acted as main supervisor and Professor Jens Nielsen and Assistant Professor Kaisa Karhumaa as cosupervisors.

Preface

This dissertation presents the results of my Ph.D. study carried out at the Center for Microbial Biotechnology (CMB), Department of Systems Biology, Technical University of Denmark, in the period from December 2006 to March 2011.

I am indebted to various people who have made my study in the center a highly joyful and inspiring time. First of all, I would like to thank my supervisors Professor Morten C. Kielland-Brandt and Assistant Professor Kaisa Karhumaa, for their guidance and encouragement in solving various problems in my research. I am also grateful to Professor Jens Nielsen and Postdoc Verena Siewers, who supervised me in the first part of my Ph.D. thesis.

Various colleagues have helped me throughout my research. I would particularly thank Irina Borodina for invaluable discussions and inspiration on my research. Jesper Mogensen and Jette Jepmond Mortensen have provided crucial technical assistance in my experimental work. Michael Rørdam Andersen has provided invaluable help in the modelling part of this work.

I would also like to acknowledge Technical University of Denmark for providing the scholarship and S.C. Van Foundation, Denmark for financing part of my Ph.D. study.

Finally, I wish to thank my family for their support and encouragement throughout my work, which has been beyond words.

Copenhagen, March 2011

Xiao Chen

Summary

Saccharomyces cerevisiae is widely used in microbial production of chemicals, metabolites and proteins, mainly because genetic manipulation of *S. cerevisiae* is relatively easy and experiences from its wide application in the existing industrial fermentations directly benefit new *S. cerevisiae*-based processes. This study has focused on metabolic engineering of the amino acid metabolism in *S. cerevisiae* for production of two types of chemicals of industrial interest.

The first chemical is δ-(L-α-aminoadipyl)–L-cysteinyl–D-valine (LLD-ACV). ACV belongs to non-ribosomal peptides (NRPs), which are synthesized by specific peptide synthetases and have a broad range of biological and pharmacological properties. Due to the scarcity of the production of NRPs in nature and the difficulties in their chemical synthesis, it was initiated here to develop *S. cerevisiae* as a platform for microbial production of one type of NRPs – ACV. Production of ACV was achieved by introducing the *Penicillium chrysogenum* gene *pcbAB*, which encodes ACV synthetase (ACVS), and the *Aspergillus nidulans* gene *npgA*, which encodes phosphopantetheinyl transferase (PPTase) required for activation of ACVS, into *S. cerevisiae* on a high-copy plasmid. Several possible factors that could improve ACV production were investigated. Lowering the cultivation temperature from 30 to 20 ^{o}C led to a 30-fold enhancement. The ACVS and PPTase encoding genes were also integrated into the yeast genome.

The second chemical is isobutanol, which is regarded as an important next generation biofuel. As a substitute for liquid fossil fuels, isobutanol is better than ethanol due to its higher energy density, lower hygroscopicity and lower vapor pressure. Isobutanol is also better than its isomer *n*-butanol due to a higer octane number. In this study, by simultaneous overexpression of biosynthetic genes *ILV2*, *ILV3*, and *ILV5* in valine metabolism in *S. cerevisiae*, the isobutanol yield was improved from 0.16 to 0.97 mg per g glucose in anaerobic fermentation in mineral medium. Isobutanol yield was further improved by two times by the additional overexpression of *BAT2*. Additional

overexpression of *ILV6* in the *ILV2 ILV3 ILV5* overexpression strain decreased isobutanol production yield by three times.

The stoichiometric genome-scale model of *S. cerevisiae* was applied to find genetic manipulation targets. The BioOpt software was used for *in silico* cell metabolism simulation. A reasonable agreement was obtained between the experimental data and the *in silico* simulation results. Through the application of single gene overexpression and deletion options of BioOpt in the overexpression strain ILV2356_XCY605, several target genes are suggested for further overexpression or deletion.

Dansk sammenfatning

Saccharomyces cerevisiae (bagegær) anvendes til mikrobiel fremstilling af en bred palet af produkter, eksempelvis kemikalier, metabolitter og proteiner. Den brede anvendelse skyldes hovedsageligt, at genmanipulation af *S. cerevisiae* er forholdsvist enkelt, samt at erfaringen fra eksisterende processer kan direkte udnyttes i nye processer baseret på *S. cerevisiae*. Nærværende studie fokuserer på manipulation af mikroorganismens omsætning af aminosyrer for at opnå produktion af to kemikalier med industriel anvendelse.

Det første stof er δ-(L-α-aminoadipyl)-L-cysteinyl-D-valin (LLD-ACV). ACV tilhører de non-ribosomale peptider (NRPer), der syntetiseres af en særlig klasse af peptid synthetaser. NRPer har beviseligt en lang række biologiske og farmakologiske aktiviteter. Grundet den lave koncentration af de enkelte NRPer i de naturlige processer og det faktum at kemisk syntese af disse stoffer er meget udfordrende, er det her blevet søgt at udvikle *S. cerevisiae* som en platform til produktion af én slags NRP: ACV. ACV-produktion i *S. cerevisiae* blev opnået ved at indsætte *pcbAB*-genet fra *Penicillium chrysogenum*, der koder for ACV synthetase (ACVS), og *npgA*-genet fra *Aspergillus nidulans*, som koder for phosphopantetheinyl transferase (PPTase). PPTase er nødvendigt for aktiveringen af ACVS. Begge gener blev overført til *S. cerevisiae* ved hjælp af et plasmid med højt kopi-tal. Et antal faktorer, der potentielt kunne påvirke productionen af ACV, blev undersøgt. Sænkning af kultiveringstemperaturen fra 30 til 20 ^{o}C øgede produktionen 30 gange. Effekten af at integrere *pcbAB* og *npgA* direkte i gærens arvemasse blev også undersøgt.

Det andet stof, der blev søgt produceret, er isobutanol – en af kandidaterne til næste generation af bio-baserede brændstoffer. Isobutanol er en bedre erstatning af flydende fossile brændstoffer end ethanol, da isobutanol har højer energitæthed, lavere vandabsorption og laver damptryk. Isobutanol er også bedre end sin isomer *n*-butanol da det har et højere oktantal. I dette studie blev isobutanol-udbyttet øget fra 0.16 til 0.97 mg/g glukose ved at overudtrykke *ILV2*, *ILV3* og *ILV5* generne fra valinstofskiftet i *S. cerevisiae*. Udbyttet blev øget ved anaerob gæring i et mineral-

baseret vækstmedium. Isobutanoludbyttet blev yderligere fordoblet ved tillige at overudtrykke *BAT2*-genet. Yderligere overekspression af *ILV6* nedsatte isobutanol produktionsudbyttet til en tredjedel.

En støkiometrisk model af stofskiftet i *S. cerevisiae* blev anvendt til at finde nye gen-kandidater til forbedring af isobutanol-produktionen. Softwaren BioOpt blev anvendt til at simulere stofskiftet *in silico* og en rimelig overenstemmelse mellem simuleringsresultaterne og data fra de anaerobe gæringer blev observeret. Anvendelse af BioOpts muligheder for forudsigelse af resultatet af deletion eller overudtryk af enkelte gener i stammen ILV2356_XCY605 identificerede et antal gener til videre studier.

Contents

Chapter 1. Introduction

Saccharomyces cerevisiae is probably the most widely used eukaryotic organism in human life. It has been used to produce fermented foods such as wine, beer and bread since acient times. Nowadays *S. cerevisiae* is broadly used in industrial biotechnology for production of a wide range of chemicals, metabolites and proteins. In addition to its application in industry, *S. cerevisiae* also serves as a model organism for modern cell biology research.

S. cerevisiae can be used to produce various metabolites of practical interest such as non-ribosomal peptides (NRPs). NRPs belong to secondary metabolites, and many of them have active biological activities and can be used for pharmaceutical purposes. They are synthesized by peptide synthetases and could contain non-proteinogenic amino acids. Natural organisms only produce NRPs in small concentrations and masss production by purficiation from those biological sources is impractical. Chemical synthesis of NRPs is also challenging due to the complexity of those peptides. Heterologous production of NRPs in *S. cerevisiae* may provide an alternative way of production of this group of compounds. In this study, the non-ribosomal tripeptide δ-(L-α-aminoadipyl)–L-cysteinyl–D-valine (LLD-ACV), which is naturally produced in most *Penicillium* species, was chosen as the model NRP, and heterologously produced in *S. cerevisiae*.

Another group of chemicals that are valuable to produce in *S. cerevisiae* are biofuels. Synthesis of biofuels from renewable resources has attracted an increasing interest these years due to the global energy and environmental problems. Bioethanol accounts for the major proportion in today's biofuel production. Compared to bioethanol, higher alcohols have a number of advantages including higher energy density, lower hydroscopicity, and lower vapour pressure, making them better substitutes for fossil fuels used in transportation. Among those higher alcohols, isobutanol is favored over *n*-butanol due to its higher octane number, and regarded as a promising type of the next generation biofuels. Since *S. cerevisiae* is the ideal

natural host for alcohol production, a study of the production of isobutanol in *S. cerevisiae* was performed in the second part of this PhD project.

The present thesis consists of six chapters. In Chapter 1 and Chapter 2, background knowledge relevant to *S. cerevisiae* cell factories, genome-scale model, etc., is described. In Chapter 3, heterologous production of non-ribosomal peptide ACV, as well as the strategies applied to improvement of the production, is investigated. The *Penicillium chrysogenum* gene *pcbAB*, which encodes ACV synthetase (ACVS), is expressed in *S. cerevisiae* from a high-copy plasmid together with phosphopantetheinyl transferase (PPTase)-encoding genes from *Aspergillus nidulans*, *P. chrysogenum* and *Bacillus subtilis*. To improve ACV synthesis, codon optimization and low-temperature cultivation were studied. An ACVS and PPTase genome integration strain was also investigated to see the effect of the copy number of the genes on the production of ACV. In Chapter 4, an experimental study was carried out to improve isobutanol production in *S. cerevisiae*. Several genes of valine biosynthetic and degradation pathways were simultaneously overexpressed with different combinations. The constructed strains were characterized on different media with glucose as the growth-limiting component during anaerobic and aerobic batch cultivations. The isobutanol concentration in the fermentation broth was measured through head-space gas chromatography (GC). In Chapter 5, further analysis of isobutanol production in *S. cerevisiae* was performed by applying an *S. cerevisiae* genome-scale model for searching other factors that would influence isobutanol production. In Chapter 6, conclusions are drawn from the previous chapters and future perspectives are presented.

Chapter 2. *Saccharomyces cerevisiae* as a cell factory

2.1. Introduction

S. cerevisiae is a budding yeast widely used in fermentation processes. It is traditionally used to produce fermented foods, such as bread and alcoholic beverages. Its modern usage is not limited to food production. It has been extended into industrial production of other chemicals, metabolites, and proteins.

S. cerevisiae is recognized today not only as an extremely useful model eukaryote organism but also as a promising cell factory for industrial applications due to its several unique features. *S. cerevisiae* can be cultured with ease on different carbon sources. It has a high growth rate with a doubling time between 1.25 and 2 hours at 30 °C (Boekhout and Robert 2003). As a eukaryote, *S. cerevisiae* has the similar internal cell structure and metabolic network with plant and animal cells, whereas its low percentage of non-coding DNA simplifies the research in molecular and cell biology in eukaryotes. In the study of the underlying mechanisms of human diseases, like cancer and diabetes, *S. cerevisiae* served as a valuable tool for being a model organism (Botstein et al. 1997; Dujon 1996). *S. cerevisiae* can be easily genetically manipulated for heterologous metabolite production and improvement of the established productions. Fermentation using *S. cerevisiae* is one of the most common types in industry and experiences with the existing processes can be applied to the production of a new chemical using *S. cerevisiae*.

Some fundamental knowledge about industrial biotechnology and metabolic engineering will be first presented below, in Sections 2.2 and 2.3. It will also be discussed why *S. cerevisiae* is a preferred organism for industrial biotechnology and metabolic engineering. Several examples of *S. cerevisiae* as a cell factory are given in Section 2.2. Application of metabolic engineering to improve production of ethanol in *S. cerevisiae* is briefly presented in Section 2.3. In connection to metabolic engineering of *S. cerevisiae*, Section 2.4 describes how a genome-scale stoichiometric model is constructed and how it works for finding target genes for production

improvement. The same type of model is used in Chapter 5 for a modeling analysis of improvement of isobutanol production. LLD-ACV production and isobutanol production in *S. cerevisiae*, which are investigated in this study, are two relatively novel processes. Some extra details about production of them in *S. cerevisiae*, not covered in Chapters 3 and 4, are given in Sections 2.5 and 2.6. Those details concern the mechanisms underlying the synthesis of the two products in *S. cerevisiae*.

2.2. Industrial biotechnology and microbial cell factories

By far, most of energy and consumer products needed in human life are produced in the chemical industry, particularly the petrochemical industry, via classical chemical synthesis. Production by chemical synthesis, however, has many drawbacks, such as substantial industrial waste, large energy consumption, and a limited range of products, often without complex structures. On the other hand, our society is faced with challenges with depleting fossil fuel reserves, growing global environmental problems, and increasing demands for energy and consumer products. New processes using renewable feedstock for bulk and fine chemical production are obviously on the agenda to decrease our dependency on the fossil fuel based economy.

Industrial biotechnology, often known as white biotechnology in Europe, provides a solution to the aforementioned challenges. The European Association for Bioindustries (http://www.europabio.org/Industrial_biotech/IB_about.htm) has defined industrial biotechnology as "the application of biotechnology for processing and production of chemicals, materials and energy" and "it uses enzymes and microorganisms to make products in sectors such as chemicals, food and feed, paper and pulp, textiles and energy".

One important aspect in industrial biotechnology is to use fermentation or enzymatic conversion processes to produce industrial useful products, replacing those produced from the traditional chemical industry. Products from the early industrial biotechnology include several important products from anaerobic fermentations, such as lactic acid, *n*-butanol and isopropanol, which can be subsequently converted to important petrochemicals, such as lactide, *n*-butylene and glycerol (Hanselman 1982).

Morden industrial biotechnology can be used to produce a larger variety of bulk and fine chemicals, such as biofuels, bioplastics, pharmaceuticals and food ingredients, from microbial fermentations rather than chemical synthesis. Biotechnological processes based on microbial cell factories have several advantages compared to the traditional chemical ones. For example, it uses sustainable bio resources instead of fossil fuels; it gives much less carbon dioxide emission and thus mitigates global warming; and it is capable of producing chemicals with a huge diversity, novel or complex structures, which are hard to obtain through chemical synthesis. A classical petrochemical process would be replaced by a microbial fermentation based biotechnological process if the latter becomes cost-effective.

Traditionally, people screened and applied the natural producer of the desired metabolites in industrial biotechnological processes. However, in recent years with the development in genetic engineering tools people tend to use several widely used microorganisms, like the filamentous fungus *Aspergillus oryzae*, the bacterium *E. coli* and the yeast *S. cerevisiae* as cell factories for production of desired products. The extensive fundamental research and the availability of numerous of genetic manipulation tools on these cell factories facilitate the ease of strain improvement and optimization of the production process (Maury et al. 2005).

S. cerevisiae is traditionally used in production of bioethanol. As a cell factory, it is also used today to produce other important chemicals including organic acids, e.g. lactic acid (Porro et al. 1999), glycerol (Geertman et al. 2006), succinate (Raab et al. 2010), and more complex natural products, e.g. vanillin, a plant secondary metabolite used as flavouring agent (Hansen et al. 2009), isoprenoids (Shiba et al. 2007), and polyketides (Mutka et al. 2006).

Another important application of *S. cerevisiae* in biotechnology is production of heterologous protein. *S. cerevisiae* is an ideal host for heterologous protein production since it can secrete protein product extracellular and post-translational modification can be performed in it (Schekman and Novick 1982). The human peptide hormone insulin produced by *S. cerevisiae* accounts for a big proportion in the current insulin market. *S. cerevisiae* is also used to produce other proteins for diagnostic purpose,

like human interferon, the hepatitis B surface antigen, papilloma virus antigen and various vaccines (Hitzeman et al. 1981; Valenzuela et al. 1982).

2.3. Metabolic engineering

Cell factories are applied extensively to industrial production processes nowadays. In order to optimize production and obtain desirable cellular properties, such as higher production yield, improved physiological properties, and production of novel metabolites, we need certain engineering tools to manipulate those cell factories. One way to achieve that is through traditional mutagenesis strategies, like random mutagenesis and screening. Although the traditional methods did provide successful cases such as production of antibiotics, solvents and vitamins (Koffas et al. 1999), they are always demanding in terms of time and labor. This is partly due to the fact that those traditional methods are not based on a systematic understanding of the underlying mechanism for the desired cellular properties. Even in the cases where the desired properties are obtained, the underlying mechanism is still largely unknown, which benefits little to the further research and development.

Metabolic engineering is defined as "the directed improvement of product formation or cellular properties through the modification of specific biochemical reactions or introduction of new ones with the use of recombinant DNA technology" (Stephanopoulos 1999). The practice of metabolic engineering can be described as an iterative process consisting of three steps: synthesis, analysis and design (Nielsen 2001). The synthesis step mainly utilizes DNA biotechnology including cloning, transformation and homologous recombination to achieve genetic modifications. The new constructed strains with the genetic modifications are then tested in the analysis step to complete their metabolic characterization. Different analytical techniques, like transcription analysis, protein analysis, metabolite analysis, and flux analysis, could be applied. Comparison with the original strain is made in their fermentation physiology and metabolic network. By interpreting the obtained analysis data, further examination of the metabolism network is made, and new genetic manipulation targets for the next round can be proposed in the design step (Nielsen 2001). Compared with the traditional random mutagenesis and screening, the most crucial

difference in metabolic engineering is that the practice of metabolic engineering is based on rational and directed genetic modifications.

Metabolic engineering helps us to improve the microbial production processes in a more efficient way. Application of metabolic engineering in biotechnological fields are mainly used to obtain higher yield or productivity of the target metabolite, improve cellular physiology for an optimized process, delete or down-regulate by-product formation, produce novel products, etc. (Stephanopoulos 1998).

In order to carry out efficient metabolic engineering in a strain improvement process, the availability of competent genetic modification tools for the given strain is necessary. Metabolic engineering can be relatively easily carried out in *S. cerevisiae* mainly due to its well-defined genetic system and highly efficient heterologous recombination feature. *S. cerevisiae* also has other advantages favourable to metabolic engineering, such as the availability of numerous markers, strains (especially auxotrophic strains) and efficient transformation vectors. *S. cerevisiae* has a high degree of homologous recombination, which facilitates modification of the yeast genome on specific locations. Furthermore, there are promoters with different strength that can control the expression level of the interested gene(s). For example, glycolytic promoters, such as *PGK1*, the promoter of the gene encoding 3-phosphoglycerate kinase, the key enzyme in glycolysis and gluconeogenesis, can be used for strong constitutive expression of the target gene(s) (Blake and Rice 1981). Regulated expression in *S. cerevisiae* could also be achieved by applying inducible promoters like *GAL*7, which is the promoter of the gene encoding galactose-1-phosphate uridyl transferase in *S. cerevisiae* galactose metabolism. The expression under the control of *GAL7* is regulated by the galactose and the glucose concentrations in the medium (Park et al. 1993).

Metabolic engineering has been extensively applied to improving production of bioethanol in *S. cerevisiae*. A central issue in bioethanol production is to lower the production price so that the produced bioethanol can be competitive with fossil fuel. Several modifications of *S. cerevisiae* have been made to address the issue. An important new feature introduced to *S. cerevisiae* is the capability of growing on

xylose, one of the main components of lignocelluloses. This is achieved by inserting genes encoding xylose isomerise from the anaerobic fungus *Piromyces* sp.E2 (Kuyper et al. 2003). In order to enhance the use of substrates, the gene encoding Mig1p DNA-binding protein was deleted to remove the suppression for metabolism of carbon sources other than glucose (Olsson et al. 1997). A major by-product in the bioethanol production using *S. cerevisiae* is glycerol. Its production was suppressed by deletion of gene *GDH1*, which encodes the NADPH-dependent glutamate dehydrogenase (Nissen et al. 2000). The aforementioned modifications based on metabolic engineering have significantly improved the bioethanol production in *S. cerevisiae*.

2.4. Genome-scale stoichiometric model of *S. cerevisiae*

Mathematical models can be used to describe the metabolisms in various organisms with some necessary assumptions or simplifications. With the help of mathematical models, their metabolisms can be analyzed for various purposes. For *S. cerevisiae*, metabolic reconstructions and constraint-based modeling are valuable tools for predicting its phenotypic behavior (Duarte et al. 2004b). The same modeling strategy is adopted here for metabolic engineering of *S. cerevisiae* amino acid metabolism for improvement of isobutanol production.

In the traditional improvement of phenotypes such as increase in the yield of a desired metabolite, it is only possible to apply the old experiences or to make analysis of small-scale metabolic pathways to select the gene targets for manipulation. After the small-scale analysis has identified the synthetic pathway or the competing pathway for the targeted metabolite, the synthetic pathway can be overexpressed and the competing one can be disrupted or reduced. In this way, more carbon is directed to the formation of the targeted metabolite. The traditional small-scale analysis, although assuming that the analyzed pathways have no interaction with the rest of the metabolic network, has achieved some successes in the past (Ostergaard et al. 2000). The choice of the small-scale model is mainly due to the lack of a modeling framework that can take into account numerous metabolic pathways and their interactions in the metabolic network. Nowadays, extensive knowledge of *S. cerevisiae* has accumulated in its cell biology and biochemistry, and its complete

genome sequence (Goffeau et al. 1996) is available, which leads to the establishment of genome-scale network models. Those models, in combination with mathematical tools like flux balance analysis (FBA) and linear programming, provide the possibility of genome-scale analysis in metabolic engineering.

The first stoichiometric genome-scale model of *S. cerevisiae* was established in 2003 (Forster et al. 2003a). Reconstruction of the metabolic network of *S. cerevisiae* involves collection of the relevant genomic, biochemical, and physiological information for *S. cerevisiae*, and inclusion of the important enzymatic reactions in the metabolic pathways of *S. cerevisiae*. The sources of information cover the genome annotation, biochemical pathway databases, biochemistry textbooks, and the latest publications by then. The reconstructed metabolic network consisted of 1175 metabolic reactions and 584 metabolites. It included 708 metabolic open reading frames (ORFs), to which 1035 reactions were assigned. It also included cofactors like NADH and NADPH into consideration. The metabolic reactions were classified into two groups in the first version: mitochondria reactions and the rest into one group as cytosolic reactions. Regulation information, however, was not included in the network due to lack of the complete regulation information, complexity of the regulation network, and difficulty of integrating the regulation information into the flux balance analysis (Forster et al. 2003a).

Several genome-scale metabolic models are now available for *S. cerevisiae*, including *iFF708*, *iND750, iLL672* and *iIN800* (Duarte et al. 2004a; Forster et al. 2003a; Kuepfer et al. 2005; Nookaew et al. 2008). All these models share a similar calculation framework. The biochemical network in *S. cerevisiae* is described by a set of stoichiometric reactions in these models (Patil et al. 2004). These reaction rates can be calculated by flux balance analysis under steady-state growth conditions (Asadollahi et al. 2009; Kauffman et al. 2003). To determine an optimum flux distribution, an objective function must be specified by the user, and linear programming is employed for the optimization with constraints (Famili et al. 2003; Forster et al. 2003b).

The genome-scale metabolic model of *S. cerevisiae* (Forster et al. 2003a) has the capability of predicting the change in phenotype due to single gene deletion. This can be used to evaluate the model by comparing the model predicted phenotypes with the experimental data. Famili et al. performed such an evaluation by simulating growth on a synthetic complete medium after single-gene deletions (Famili et al. 2003; Forster et al. 2003b). It was found that 81.5% (93 of 114 cases) of the *in silico* predictions were in agreement with *in vivo* phenotypes (Famili et al. 2003; Forster et al. 2003b). A larger-scale investigation of *in silico* gene deletion was performed later (Famili et al. 2003; Forster et al. 2003b), where 599 mutant strains of *S. cerevisiae* were included in the comparison. It was found that 87.8% (526 of 599 cases) of the *in silico* results were in agreement with the experimental observations when growth on synthetic medium was simulated. These two evaluations showed the capability of the model to reproduce most of the existing data for *S. cerevisiae* and also the potential usage of the model in understanding and predicting the metabolic behavior of *S. cerevisiae* (Famili et al. 2003; Forster et al. 2003b).

Genome-scale metabolic models of *S. cerevisiae* can be used to guide the design of an improved *S. cerevisiae* cell factory. One recent application of the genome-scale metabolic model of *S. cerevisiae* (Forster et al. 2003a) is to enhance sesquiterpene production in *S. cerevisiae* through *in silico* driven metabolic engineering (Asadollahi et al. 2009). The authors used the stoichiometric model of *S. cerevisiae* to evaluate the effect of gene deletions on sesquiterpene production by using OptGene with minimization of metabolic adjustments (MOMA) as objective function. The analysis showed that deletion of NADPH-dependent glutamate dehydrogenase encoded by *GDH1* was the best target for the further experimental study. For this mutant, the model prediction gives around 10-fold increase in the flux towards sesquiterpene production, with 15% reduction in the specific growth rate. The experimental results in 5 L batch two-phase fermenters showed an approximately 85% increase in the final sesquiterpene concentration and a significant decrease (65%) in the maximum specific growth rate, which were in general agreement with the model predictions although the increase in the sesquiterpene production was moderate and the reduction in specific growth rate was much higher. The authors argued that it was due to the fact that stoichiometric models do not take into account of the kinetic and thermodynamic

constraints on the possible flux changes. Despite the limitations, the directions of the changes were correctly predicted. Another example of application of the *S. cerevisiae* model in *in silico* design is the improvement of production of vanillin through a heterologous introduced pathway (Brochado et al. 2010). In that study, *iFF708* was employed to identify and select target reactions by using OptGene with MOMA as the biological objective function. Among six reaction knockout targets, two targets (*PDC1* and *GDH1*) were finally selected for experimental verification. In the experiments with the modified strains, a 1.5-fold higher vanillin β-D-glucoside yield in batch fermentation was achieved for three different mutants and a 2-fold productivity improvement in continuous culture for the *Δpdc1* mutant. The study demonstrates again that use of the genome-scale metabolic model of *S. cerevisiae* can guide the design of overproducing strains.

2.5. Non-ribosomal peptide LLD-ACV biosynthesis

Tripeptide δ-(L-α-aminoadipyl)–L-cysteinyl–D-valine (LLD-ACV) is a type of non-ribosomal peptides (NRPs) and the starting point for β-lactam antibiotic biosynthesis. NRPs are small peptide molecules synthesized independent of DNA sequence, and often contain unusual amino acids as building blocks. People have shown great interest in NRPs mainly because most of them have active biological activities, and could be used for pharmaceutical purpose (Sieber and Marahiel 2005).

Synthesis of NRPs is controlled by non-ribosomal peptide synthetases (NRPS), in contrast to the synthesis of other common proteins by ribosome. The synthesis mechanism of NRPs belongs to the multienzyme thiotemplate mechanism (Sieber and Marahiel 2005). The multienzyme complex NRPS can be divided into different modules. Each module is responsible for taking one specific amino acid into the peptide product (Sieber and Marahiel 2005). A module can be subdivided into a number of domains. Different domains have different individual enzymatic functions, such as substrate recognition and activation, binding, modification, elongation, and release. NRPS works as a template and biosynthetic machinery during the peptide synthesis process. Different domains in each module contribute to the amino acid addition to the peptide chain, and after the addition of all of the amino acid molecules,

the final peptide product is checked and the one with the right structure is released from the complex (Sieber and Marahiel 2005). The features of NRPs are determined by the order and the characteristics of the domains. Therefore it is possible to make the enzyme with totally new features by domain shuffling (Sieber and Marahiel 2005).

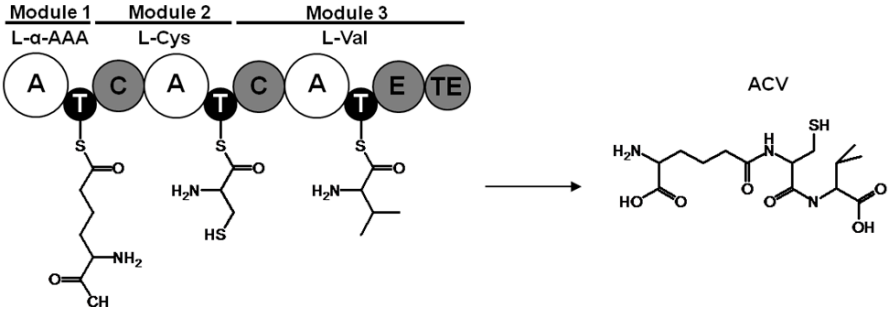

Figure 2.1. Synthesis of ACV by ACV synthetase: andenylation domain (A domain), thiolation domain (T domain), condensation domain (C domain), epimerization domain (E domain), and thioesterase domain (TE domain) (Figure from Verena Siewers, unpublished).

Synthesis of the tripeptide ACV by a single multifunctional enzyme ACV synthetase (ACVS) is illustrated in Figure 2.1. ACV is formed through the condensation of three amino acids, L-α-aminoadipic acid, L-cysteine and L-valine, and the subsequent epimerization of the L-valine to D-valine (Brakhage 1998). The ACVS consists of three modules, which are responsible for activation, thiolation, and condensation of each amino acid. Those modules are made of several functional domains: andenylation domain (A domain), thiolation domain (T domain)—also known as the peptidyl carrier protein (PCP), condensation domain (C domain), epimerization domain (E domain), and thioesterase domain (TE domain). During the synthesis, the A domains on different modules first recognize and activate their corresponding amino acids from a pool of substrates. Catalyzed by the enzyme in this step, the activated amino acids are converted to aminoacyl adenylate intermediates. The intermediates are transferred to the free thiol group of a 4'-phosphopantetheinyl cofactor (ppan) bound to T domains (or PCPs). The T domains, located downstream of the corresponding A domains, are the only non catalytic domains. Peptide elongation is achieved by the C domains, which catalyze an attack of the nucleophillic amine of the building block in the downstream onto the electrophilic thioester of the

building block in the upstream (Sieber and Marahiel 2005). The last module in ACVS contains an E domain which converts L-valine to its D-isomer. The peptide grows from the amino terminus to the carboxyl terminus, and the intermediate peptides keep bound to the enzyme (Kleinkauf and Von Dohren 1996). Once the assembly line of the amino acids is ended, the formed peptide is released at the C-terminal TE domain of the enzyme. The TE domain at the C-terminal region of ACV synthetase is responsible for the selective release of tripeptide with the correct LLD configuration (Kleinkauf and Von Dohren 1996). This highly ordered process is beneficial in preventing side reactions and saving time for substrate transportation (Sieber and Marahiel 2005).

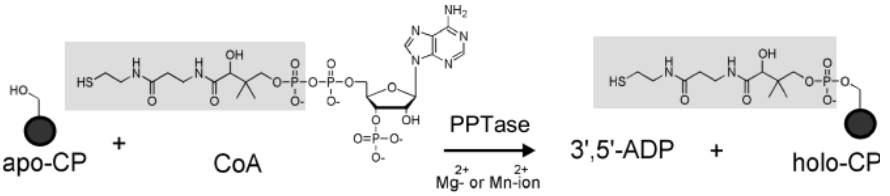

Figure 2.2. Activation reaction of T domain of NRPS by PPTase. In the presence of Mg^{2+} or Mn^{2+} ions, the T domain (PCP) is activated from their inactive apo form to the active holo form by transfer of a 4'-phosphopantetheinyl moiety from coenzyme A onto the hydroxyl side chain of a conserved serine residue of the CP (Figure from Mofid et al. 2004).

In addition to ACVS, another enzyme 4'-phosphopantetheinyl transferase (PPTase) is needed in the synthesis of ACV. The post-translational addition of the 4'-phosphopantetheinyl moiety (P-pant) onto the T domain (PCP) of NRPS is required for covalent capture of amino acids which is activated by A domain. This activation of PCP from the inactive apo-form to functionally active holo-PCP is accomplished through catalysis by PPTase. In the presence of Mg^{2+} or Mn^{2+} ions, the hydroxyl side chain of the highly conserved serine residue of the T domain (PCP) attacks the 5'-β-phosphate of CoA, thus releasing active holo form of PCP and 3', 5'- ADP (Figure 2.2) (Mofid et al. 2004).

2.6. Production of branched-chain higher alcohols in *S. cerevisiae*

Two challenging issues that mankind are confronted with today are the energy security and the global climate change. With the increasing global demand for energy and the limited reserves of fossil fuels, the role of sustainable energy in the whole energy portfolio becomes bigger and bigger. Replacement of fossil fuels by sustainable energy can also reduce CO_2 emission and mitigate the greenhouse gas effects. Among various types of sustainable energy, liquid biofuels, produced from biomass, have received enormous attention, largely because it is by far the only option implemented on a large scale to substitute liquid fossil fuels used in transportation. Major types of liquid biofuels include bioalcohols, vegetable oils, and biodiesel. Bioethanol production is the most matured technology among various liquid biofuels. Bioethanol has been produced in large amounts from feedstocks such as corn or sugar cane for years, and recently lignocelluslosic bioethanol production started from woody or fibrous biomass which cannot be used as food. Actually, higher alcohols with longer carbon chains may have more suitable properties than ethanol as substitutes for the current fossil fuels. Butanols have four different isomers, *n*-butanol (1-butanol or butan-1-ol), isobutanol (isobutyl alcohol or 2-methylpropan-1-ol), 2-butanol (sec-butanol or butan-2-ol) and *t*-butanol (tert-butanol or 2-methyl-propan-2-ol). In general all these four isomers have a higher energy density, lower hygroscopicity, and lower vapor pressure than ethanol. As a result, butanols provide energy content closer to that of gasoline than ethanol, better water stability and smaller tendency to separation when blended with gasoline, and does not increase the vapor pressure when added to gasoline. The aforementioned advantages also facilitate the use of the existing fuel distribution infrastructure for biobutanols.

Biological synthesis of butanol is by far mainly achieved by the Acetone Butanol Ethanol (ABE) fermentation process using the *Clostridia* bacteria such as *Clostridium acetobutylicum*. The process utilizes feedstock such as wheat and corn and produces acetone, 1-butanol and ethanol together. The process was largely replaced by more economic petrochemical processes during the 1950s. Recently, a renewed interest in this process as well as other ways to produce biobutanols has appeared, driven by the high oil prices and the demands in chemical markets (Butamax^{TM} Advanced Biofuels

LLC January 2010). In 2006, North American based company DuPont and UK based company BP created a partnership to develop, produce and market the next generation biofuels, with focus on biobutanols. While BP and DuPont are working on different butanol isomers, it is isobutanol that they have selected for commercialization (Butamax^{TM} Advanced Biofuels LLC January 2010). Compared to *n*-butanol, isobutanol has a higher octane number and is more suitable as biofuel. Recently, the research group led by J.C. Liao at University of California, Los Angeles, has engaged in using engineered *Escherichia coli* to produce different higher alcohols, including isobutanol (Atsumi et al. 2008a; Atsumi et al. 2008b; Hanai et al. 2007; Shen and Liao 2008). The isobutanol concentration reportedly reached 22 g/L during aerobic cultivations (Atsumi et al. 2008). However, compared with yeasts, *E. coli* is less robust against pH or temperature change, and has a lower alcohol tolerance (Weber et al. 2010), which can be a potential limitation in its industrial applications. Production of isobutanol with yeast like *S. cerevisiae* seems to be more suitable especially because isobutanol is already produced by wild-type *S. cerevisiae* (Weber et al. 2010). Actually, several companies like DuPont, Gevo and Butalco are working on the genetic engineering of *S. cerevisiae* for isobutanol production although no scientific articles have yet been published in this area (Weber et al. 2010). It should be mentioned that we were not aware of the fact until the late stage of this study.

The biosynthetic pathway of higher branched alcohols in *S. cerevasiae* is illustrated in Figure 2.3. Metabolism of amino acid in *S. cerevasiae* generates 2-keto acids as intermediates, which are converted to aldehydes by broad-substrate-range decarboxylases and then to alcohols by alcohol dehydragenases (ADHs) (Figure 2.3a). Figure 2.3b illustrates four different branched-chain higher alcohols production in *S. cerevasiae*. The biosynthesis pathways for four different amino acids, including valine, isoleucine, leucine, and pheylalanine, produce 2-keto-isovalerate, 2-keto-3-methyl-valerate, α-ketoisocaproate, and phenylpyuvate, respectively. These four 2-keto acids are then converted to isobutanol, 2-methyl-1-butanol, 3-methyl-1-butanol, and 2-phenylethanol, respectively.

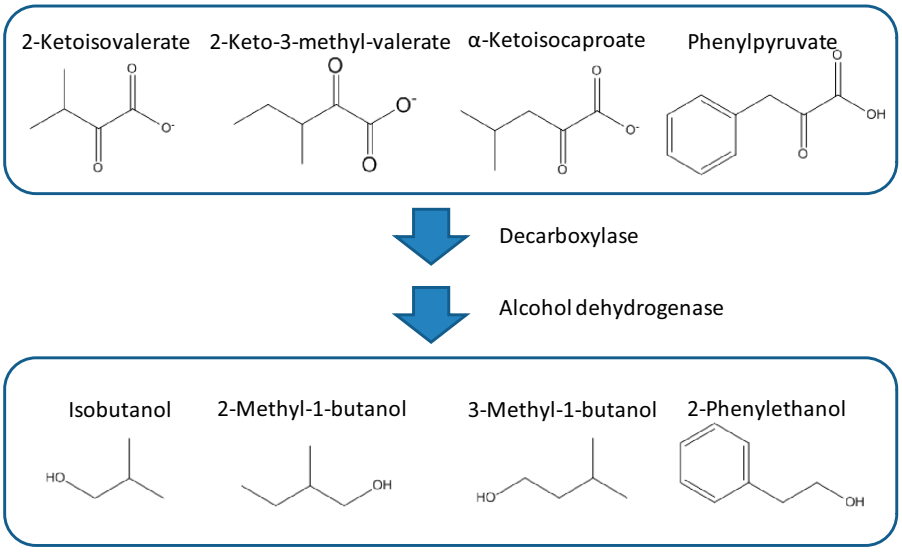

(a)

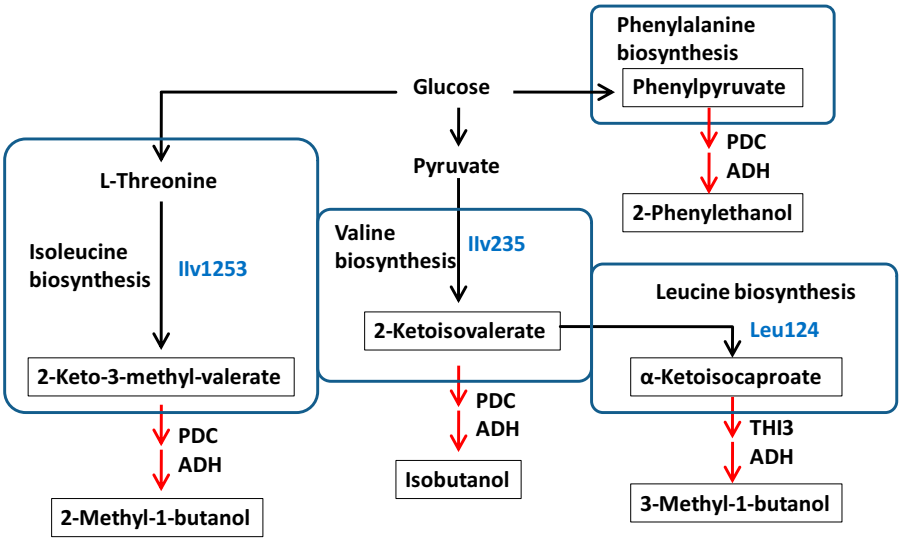

(b)

Figure 2.3. Biosynthesis of higher alcohols in *S. cerevisiae*: (a) various 2-keto acid precursors converted to corresponding alcohols by decarboxylase and alcohol dehydrogenase; (b) various amino acid biosynthesis pathways lead to production of higher alcohols in *S. cerevisiae* (modified from Atusmi et al. 2008b).

2.7. Summary

This chapter has covered diverse topics as background and fundamentals for the following chapters. It starts with a general description about the importance of industrial biotechnology and microbial cell factories to our society and the significance of metabolic engineering to modern biotechnology. In particular, examples are given to show what *S. cerevisiae* can produce as cell factories and how metabolic engineering can be used to improve production of bioethanol in *S. cerevisiae*. Furthermore, genome-scale stoichiometric modeling, as an important and unique tool in metabolic engineering, provides the possibility to analyze the cellular metabolism as a whole. Its construction and applications are therefore briefly reviewed. Background details about production of LLD-ACV and bioisobutanol, two chemicals selected in this study, have been provided. For biosynthesis of LLD-ACV, two enzymes ACVS and PPTase are essential. For bioisobutanol, its biosynthesis pathway in *S. cerevisiae* has been illustrated.

References

Asadollahi MA, Maury J, Patil KR, Schalk M, Clark A, Nielsen J. 2009. Enhancing sesquiterpene production in Saccharomyces cerevisiae through in silico driven metabolic engineering. Metab Eng 11(6):328-34.

Atsumi S, Cann AF, Connor MR, Shen CR, Smith KM, Brynildsen MP, Chou KJ, Hanai T, Liao JC. 2008a. Metabolic engineering of Escherichia coli for 1-butanol production. Metab Eng 10(6):305-11.

Atsumi S, Hanai T, Liao JC. 2008b. Non-fermentative pathways for synthesis of branched-chain higher alcohols as biofuels. Nature 451(7174):86-9.

Blake CC, Rice DW. 1981. Phosphoglycerate kinase. Philos Trans R Soc Lond B Biol Sci 293(1063):93-104.

Boekhout T, Robert V, editors. 2003. Yeasts in Food: Beneficial and Detrimental Aspects. Hamburg: B. Behr's Verlag GmbH & Co.

Botstein D, Chervitz SA, Cherry JM. 1997. Yeast as a model organism. Science 277(5330):1259-60.

Brakhage AA. 1998. Molecular regulation of beta-lactam biosynthesis in filamentous fungi. Microbiol Mol Biol Rev 62(3):547-85.

Brochado AR, Matos C, Moller BL, Hansen J, Mortensen UH, Patil KR. 2010. Improved vanillin production in baker's yeast through in silico design. Microb Cell Fact 9:84.

Butamax^{TM} Advanced Biofuels LLC. January 2010. California Biobutanol Multimedia Evaluation Tier I Report.

Duarte NC, Herrgard MJ, Palsson BO. 2004a. Reconstruction and validation of Saccharomyces cerevisiae iND750, a fully compartmentalized genome-scale metabolic model. Genome Res 14(7):1298-309.

Duarte NC, Palsson BO, Fu P. 2004b. Integrated analysis of metabolic phenotypes in Saccharomyces cerevisiae. BMC Genomics 5:63.

Dujon B. 1996. The yeast genome project: what did we learn? Trends Genet 12(7):263-70.

Famili I, Forster J, Nielsen J, Palsson BO. 2003. Saccharomyces cerevisiae phenotypes can be predicted by using constraint-based analysis of a genome-scale reconstructed metabolic network. Proc Natl Acad Sci U S A 100(23):13134-9.

Forster J, Famili I, Fu P, Palsson BO, Nielsen J. 2003a. Genome-scale reconstruction of the Saccharomyces cerevisiae metabolic network. Genome Res 13(2):244-53.

Forster J, Famili I, Palsson BO, Nielsen J. 2003b. Large-scale evaluation of in silico gene deletions in Saccharomyces cerevisiae. OMICS 7(2):193-202.

Geertman JM, van Maris AJ, van Dijken JP, Pronk JT. 2006. Physiological and genetic engineering of cytosolic redox metabolism in Saccharomyces cerevisiae for improved glycerol production. Metab Eng 8(6):532-42.

Goffeau A, Barrell BG, Bussey H, Davis RW, Dujon B, Feldmann H, Galibert F, Hoheisel JD, Jacq C, Johnston M and others. 1996. Life with 6000 genes. Science 274(5287):546, 563-7.

Hanai T, Atsumi S, Liao JC. 2007. Engineered synthetic pathway for isopropanol production in Escherichia coli. Appl Environ Microbiol 73(24):7814-8.

Hanselman KW. 1982. Lignochemicals. Experientia 38:176-189.

Hansen EH, Moller BL, Kock GR, Bunner CM, Kristensen C, Jensen OR, Okkels FT, Olsen CE, Motawia MS, Hansen J. 2009. De novo biosynthesis of vanillin in fission yeast (Schizosaccharomyces pombe) and baker's yeast (Saccharomyces cerevisiae). Appl Environ Microbiol 75(9):2765-74.

Hitzeman RA, Hagie FE, Levine HL, Goeddel DV, Ammerer G, Hall BD. 1981. Expression of a human gene for interferon in yeast. Nature 293(5835):717-22.

Kauffman KJ, Prakash P, Edwards JS. 2003. Advances in flux balance analysis. Curr Opin Biotechnol 14(5):491-6.

Kleinkauf H, Von Dohren H. 1996. A nonribosomal system of peptide biosynthesis. Eur J Biochem 236(2):335-51.

Koffas M, Roberge C, Lee K, Stephanopoulos G. 1999. Metabolic engineering. Annu Rev Biomed Eng 1:535-57.

Kuepfer L, Sauer U, Blank LM. 2005. Metabolic functions of duplicate genes in Saccharomyces cerevisiae. Genome Res 15(10):1421-30.

Kuyper M, Harhangi HR, Stave AK, Winkler AA, Jetten MS, de Laat WT, den Ridder JJ, Op den Camp HJ, van Dijken JP, Pronk JT. 2003. High-level functional expression of a fungal xylose isomerase: the key to efficient ethanolic fermentation of xylose by Saccharomyces cerevisiae? FEMS Yeast Res 4(1):69-78.

Maury J, Asadollahi MA, Moller K, Clark A, Nielsen J. 2005. Microbial isoprenoid production: an example of green chemistry through metabolic engineering. Adv Biochem Eng Biotechnol 100:19-51.

Mofid MR, Finking R, Essen LO, Marahiel MA. 2004. Structure-based mutational analysis of the 4'-phosphopantetheinyl transferases Sfp from Bacillus subtilis: carrier protein recognition and reaction mechanism. Biochemistry 43(14):4128-36.

Mutka SC, Bondi SM, Carney JR, Da Silva NA, Kealey JT. 2006. Metabolic pathway engineering for complex polyketide biosynthesis in Saccharomyces cerevisiae. FEMS Yeast Res 6(1):40-7.

Nielsen J. 2001. Metabolic engineering. Appl Microbiol Biotechnol 55(3):263-83.

Nissen TL, Kielland-Brandt MC, Nielsen J, Villadsen J. 2000. Optimization of ethanol production in Saccharomyces cerevisiae by metabolic engineering of the ammonium assimilation. Metab Eng 2(1):69-77.

Nookaew I, Jewett MC, Meechai A, Thammarongtham C, Laoteng K, Cheevadhanarak S, Nielsen J, Bhumiratana S. 2008. The genome-scale metabolic model iIN800 of Saccharomyces cerevisiae and its validation: a scaffold to query lipid metabolism. BMC Syst Biol 2:71.

Olsson L, Larsen ME, Ronnow B, Mikkelsen JD, Nielsen J. 1997. Silencing MIG1 in Saccharomyces cerevisiae: effects of antisense MIG1 expression and MIG1 gene disruption. Appl Environ Microbiol 63(6):2366-71.

Ostergaard S, Olsson L, Nielsen J. 2000. Metabolic engineering of Saccharomyces cerevisiae. Microbiol Mol Biol Rev 64(1):34-50.

Park YS, Shiba S, Lijima S, Kobayashi T, Hishinuma F. 1993. Comparison of three different promoter systems for secretory alpha-amylase production in fed-batch cultures of recombinant Saccharomyces cerevisiae. Biotechnol Bioeng 41(9):854-61.

Patil KR, Akesson M, Nielsen J. 2004. Use of genome-scale microbial models for metabolic engineering. Curr Opin Biotechnol 15(1):64-9.

Porro D, Bianchi MM, Brambilla L, Menghini R, Bolzani D, Carrera V, Lievense J, Liu CL, Ranzi BM, Frontali L and others. 1999. Replacement of a metabolic pathway for large-scale production of lactic acid from engineered yeasts. Appl Environ Microbiol 65(9):4211-5.

Raab AM, Gebhardt G, Bolotina N, Weuster-Botz D, Lang C. 2010. Metabolic engineering of Saccharomyces cerevisiae for the biotechnological production of succinic acid. Metab Eng 12(6):518-25.

Schekman R, Novick P. 1982. The secretory process and yeast cell-surface assembly. In: Strathern JN, editor. The molecular biology of the yeast Saccharomyces. N. Y.: Cold Spring Harbor Laboratory. p 361-393.

Shen CR, Liao JC. 2008. Metabolic engineering of Escherichia coli for 1-butanol and 1-propanol production via the keto-acid pathways. Metab Eng 10(6):312-20.

Shiba Y, Paradise EM, Kirby J, Ro DK, Keasling JD. 2007. Engineering of the pyruvate dehydrogenase bypass in Saccharomyces cerevisiae for high-level production of isoprenoids. Metab Eng 9(2):160-8.

Sieber SA, Marahiel MA. 2005. Molecular mechanisms underlying nonribosomal peptide synthesis: approaches to new antibiotics. Chem Rev 105(2):715-38.

Stephanopoulos G. 1998. Metabolic engineering. Biotechnol Bioeng 58(2-3):119-20.

Stephanopoulos G. 1999. Metabolic fluxes and metabolic engineering. Metab Eng 1(1):1-11.

Valenzuela P, Medina A, Rutter WJ, Ammerer G, Hall BD. 1982. Synthesis and assembly of hepatitis B virus surface antigen particles in yeast. Nature 298(5872):347-50.

Weber C, Farwick A, Benisch F, Brat D, Dietz H, Subtil T, Boles E. 2010. Trends and challenges in the microbial production of lignocellulosic bioalcohol fuels. Appl Microbiol Biotechnol 87(4):1303-15.

Chapter 3. Heterologous production of the non-ribosomal peptide LLD-ACV in *Saccharomyces cerevisiae*

Verena Siewers, Xiao Chen, Le Huang, Jie Zhang, and Jens Nielsen*

***Metabolic Engineering* 11** (2009) 391-397

Abstract

Non-ribosomal peptides (NRPs) are a diverse family of secondary metabolites with a broad range of biological activities. We started to develop a eukaryotic microbial platform based on the yeast *Saccharomyces cerevisiae* for heterologous production of NRPs using δ-(L-α-aminoadipyl)-L-cysteinyl-D-valine (ACV) as a model NRP. The *Penicillium chrysogenum* gene *pcbAB* encoding ACV synthetase was expressed in *S. cerevisiae* from a high copy plasmid together with phosphopantetheinyl transferase (PPTase) encoding genes from *Aspergillus nidulans*, *P. chrysogenum* and *Bacillus subtilis*, and in all the three cases production of ACV was observed. To improve ACV synthesis, several factors were investigated. Codon optimization of the 5' end of *pcbAB* did not significantly increase ACV production. However, a 30-fold enhancement was achieved by lowering the cultivation temperature from 30 to 20 ºC. When ACVS and PPTase encoding genes were integrated into the yeast genome a 6-fold decrease in ACV production was observed indicating that gene copy number was one of the rate-limiting factors for ACV production in yeast.

Keywords: secondary metabolites; non-ribosomal peptide synthetase; phosphopantetheinyl transferase; *S. cerevisiae*

3.1. Introduction

Non-ribosomal peptides (NRPs) represent a versatile group of microbial secondary metabolites exhibiting a broad range of biological and pharmacological activities (Sieber and Marahiel, 2005). They include antibiotics such as bacitracin (Eppelmann et al., 2001) and vancomycin (van Wageningen et al., 1998), antibiotic precursors like δ-(L-α-aminoadipyl)-L-cysteinyl-D-valine (ACV) (Byford et al., 1997), cytostatics such as epothilone (Molnar et al., 2000), immunosuppressive agents like cyclosporine (Weber and Leitner, 1994) and siderophores (Quadri et al., 1998a). Non-ribosomal peptides are synthesized by specific peptide synthetases via a thiotemplate mechanism (Kleinkauf and von Doehren, 1996). Unlike DNA-encoded peptides, the non-ribosomal peptides can contain non-proteinogenic amino acids, and often carry unusual modifications like *N*-methyl and *N*-formyl groups (Schwarzer et al., 2003).

Non-ribosomal peptides have attained much interest because of their important roles as human pharmaceuticals. Because of the scarcity of non-ribosomal peptide production in nature and the complexity of their structures, mass production by purification from biological material or chemical synthesis is, however, rarely performed. Moreover, it is also often difficult to genetically manipulate the natural producers for either production optimization through metabolic engineering or novel chemical entity exploration through combinatorial biosynthesis.

For these reasons we initiated the development of a yeast platform based on *Saccharomyces cerevisiae* for heterologous production of NRPs. As a model eukaryote, *S. cerevisiae* is one of the most thoroughly studied organisms. It is easy to manipulate and cultivate, and classified as a generally recognized as safe (GRAS) organism for production of a number of different products. To establish NRP production in yeast, we chose the non-ribosomal tripeptide δ-(L-α-aminoadipyl)-L-cysteinyl-D-valine (ACV) as our target in this study.

ACV is the first intermediate in the biosynthetic pathways of β-lactam antibiotics, of which the penicillins and cephalosporins are the most well-known. The formation of ACV is catalyzed by a single non-ribosomal peptide synthetase named ACV

synthetase (ACVS), which consists of three modules involved in incorporation of the corresponding amino acids L-α-aminoadipic acid, L-cysteine and L-valine, respectively. Each module is comprised of functional domains for amino acid activation, thiolation, and condensation. In addition, the last module of ACV synthetase contains an epimerization domain involved in conversion of L-valine to its D-isomer. The thioesterase domain in the C-terminal region of ACV synthetase is responsible for the selective release of the tripeptide with the correct LLD configuration (Kleinkauf and von Doehren, 1996).

In addition, a 4'-phosphopantetheinyl transferase (PPTase) is required to convert the ACVS apo-enzyme into its active form by transferring a phosphopantetheinyl moiety from coenzyme A to the conserved serine residue in carrier proteins of the three PCP domains in ACVS (Keszenman-Pereyra et al., 2003). Based on their sequence and substrate specificity, PPTases are generally classified into three types: AcpS-type PPTases associated with fatty acid synthase of prokaryotes, FAS2-type PPTases, which represent integrated domains of fatty acid synthase of eukaryotes and Sfp-type PPTases, which are usually involved in secondary metabolism (Fichtlscherer et al., 2000; Lambalot et al., 1996; Quadri et al., 1998b). The PPTases identified in *S. cerevisiae* include Lys5 involved in lysine biosynthesis, Ppt2 specific for mitochondrial acyl carrier protein (Ehmann et al., 1999), and the integrated PPTase in the fatty acid synthase responsible for its own modification (Fichtlscherer et al., 2000), which do not seem suitable for secondary metabolite production (Kealey et al., 1998). Therefore, Sfp-type PPTase encoding genes *npgA* from *Aspergillus nidulans* reported to be essential for penicillin biosynthesis (Keszenman-Pereyra et al., 2003), *sfp* from *B. subtilis*, which had been proven to be a suitable candidate for heterologous co-expression with non-ribosomal peptide and polyketide synthase genes (Quadri et al., 1998b), and *pptA* from *P. chrysogenum* (Schoergendorfer and Kurnsteiner, 2005), the same origin as *pcbAB*, the ACVS encoding gene used in this study, were chosen to be co-expressed with *pcbAB* to ensure activation of the NRPS enzyme.

In the present work, we demonstrate for the first time the production of a non-ribosomal peptide in yeast.

3.2. Materials and methods

3.2.1. Strains and growth conditions

Strains used in this study are listed in Table 3.1a. Plasmid carrying strains were maintained in synthetic dextrose (SD) minimal medium containing 6.7 g/l of yeast nitrogen base w/o amino acids (Difco Laboratories, Sparks, MD, USA), 0.6 g/l complete supplement mixture (CSM; w/o histidine, leucine, tryptophane, uracil) (MP Biomedicals, Solon, OH, USA), and 2% glucose and supplemented with 20 mg/l histidine, 60 mg/l leucine, 40 mg/l tryptophane and/or 20 mg/l uracil when appropriate. For gene induction, strains were grown in synthetic galactose (SG) minimal medium (SD medium containing 2% galactose instead of glucose) in baffled shake flasks at 150 rpm.

Table 3.1a. Yeast strains used in this study

Strain	Genotype	Reference
S. cerevisiae CEN.PK113-5D	*MAT***a** *MAL2-8*^{c} *SUC2 ura3-52*	P. Kötter, University of Frankfurt, Germany
S. cerevisiae CEN.PK113-9D	*MAT***a** *MAL2-8*^{c} *SUC2 ura3-52 trp1-289*	P. Kötter, University of Frankfurt, Germany

3.2.2. Plasmid contructions

The strategy implemented to construct the plasmids used in this study is illustrated in Figure 3.1. Gene *npgA* was amplified from plasmid pDKP4832 using primers npg-1 and npg-2. The 3' end (0.9 kb) and the 5' end (3 kb) of *pcbAB* were amplified from cosmid pCX3.2 (Smith et al., 1990; both pDKP4832 and pCX3.2 were kindly donated by G. Turner, University of Sheffield. UK) using primer pairs pcbAB-2/pcbAB-4 and pcbAB-1/pcbAB-3, respectively. All three fragments were subsequently cloned into pESC-URA (Stratagene, La Jolla, CA, USA). The resulting plasmid was linearized with *Bgl*II. In addition, a 12 kb *Spe*I fragment containing the full length *pcbAB* gene was isolated from cosmid pCX3.2. Both fragments were co-transformed into *S. cerevisiae* CEN.PK113-5D, thus allowing the formation of vector pESC-npgA-pcbAB by homologous recombination.

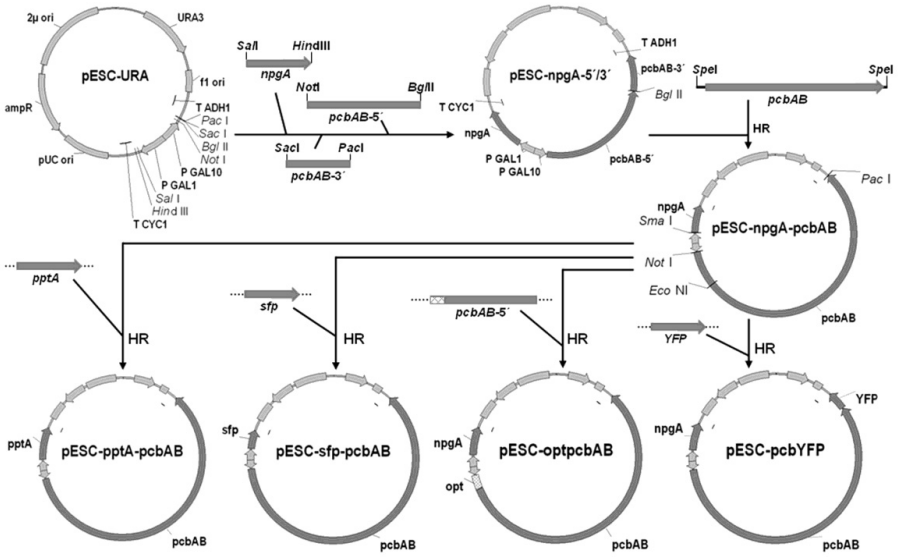

Figure 3.1. Plasmid construction. PCR product tails homologous to vector sequences are indicated as dotted lines, the codon optimized 5' end of pcbAB by a checked bar. Cloning steps that involved homologous recombination in yeast are marked as "HR". See materials and methods for further details.

cDNA of *pptA* from *P. chrysogenum* NN P8 (kindly donated by Novo Nordisk, Copenhagen, Denmark) was generated by means of RT-PCR using primer pair pptA-F/pptA-R; *sfp* was amplified from *B. subtilis* DSM3256 genomic DNA using primer pair sfp-F/sfp-R. Both primer pairs contain tails, which are homologous to the vector sequences flanking *npgA* in pESC-npgA-pcbAB. *NpgA* in this vector was replaced with *pptA* and *sfp*, respectively, by linearizing pESC-npgA-pcbAB with *Sma*I and transforming it into CEN.PK113-9D together with the respective PCR fragment. Hereby, plasmids pESC-pptA-pcbAB and pESC-sfp-pcbAB were formed by homologous recombination.

Primers pcbAB-F and module1-R were used to amplify the 5' end (2.8 kb) of *pcbAB*, thereby optimizing the first 27 codons of the gene with regard to the yeast codon bias. Plasmid pESC-npgA-pcbAB was cut with *Not*I/*Eco*NI in order to eliminate the original 5' region. Vector and PCR fragment were co-transformed into CEN.PK113-9D to generate pESC-optpcbAB by homologous recombination as described above.

Table 3.1b. Primer sequences [a]

Primer name	Sequence
npg-1	GGC**GTCGAC**ATGGTGCAAGACACATCAAGC
npg-2	CC**AAGCTT**ATTAGGATAGGCAATTACACAC
pcbAB-1	AGG**GCGGCCGC**AATGACTCAACTGAAGCCACCG
pcbAB-2	TTG**TTAATTAA**GTCAATAGCGAGCGAGGTGTTC
pcbAB-3	AGACACGTGAAGCGATTCTCG
pcbAB-4	TTCCTTAAGCGCTGCTGTCAG
pptA-F	TCACTATAGGGCCCGGGCGTCGACATGGTAGACCCAAGTGT GTCTGGA
pptA-R	TAGCTAGCCGCGGTACCAAGCTTATTAAAAGCTTGGTAAAT CCCGTAG
sfp-F	CCGTAATACGACTCACTATAGGGCATGAAGATTTACGGAAT TTATATG
sfp-R	TAGCTAGCCGCGGTACCAAGCTTATTATAAAAGCTCTTCGT ACGAG
pcbAB-F	AACCCTCACTAAAGGGCGGCCGCAATGACTCAATTGAAAC CACCAAATGGTACTACTCCAATTGGTTTTTCTGCTACTACAT CTTTGAATGCTAGTGGTAGTTCTAGTGTGAAAAATGGG
module1-R	GTCGCATTTCTCCTGCTGCTTGTT
pcbYFP-F	ATCAAGGAACACCTCGCTCGCTATGCTGAAGCTGCTGCTAA AGCTATGAGTAAAGGAGAAGAACTTTTC
pcbYFP-R	ACCAAACCTCTGGCGAAGAATTGTTAATTAATTATTTGTAT AGTTCATCCATGC
RFP-F	ATTGCC**ACTAGT**ATGGCCTCCTCCGAGGACGT
RFP-R	ACATGA**TTAATTAA**TTACAATTTAGAGGCGCCGGTGGAGT GGC
P4	GTTGCCGCAAACCAAAAA
Pxc024	CTCGAAGATCCAGCTGCATTTGTTGGGATTCCATTGTTGA
Pxc016	AATGCAGCTGGATCTTCGAG
Pxc017	GTAACCTGGCCCCACAAACC
Pxc018	CTCAACGGACTGGACAGCTT
Pxc019	CTACCCAGAATCACGATCCCATTACGCCAGCTGAATTGGA
Pxc20	GGGATCGTGATTCTGGGTAG
Pxc21	TGTGATTATCGTTGGGTCCAGTTTTCCCAGTCACGACGTT
Pxc22	TGGACCCAACGATAATCACA
Pxc23	TTCATTGGTCCTGTTGATGG

[a] Introduced restriction sites are indicated in bold.

The YFP encoding gene was amplified from plasmid pWJ1164 (Reid et al., 2002) using primers pcbYFP-F and pcbYFP-R, thereby introducing a short linker sequence in front of the YFP start codon. Plasmids pESC-npgA-pcbAB and pESC-optpcbAB were linearised by restriction with *Pac*I and transformed into CEN.PK113-9D together with the PCR fragment. The tails added to both PCR primers allowed the formation of plasmids pESC-pcbYFP and pESC-optpcbYFP by homologous recombination.

Primers RFP-F and RFP-R were used to amplify the RFP encoding DNA sequence from plasmid pWJ1350 (Lisby et al., 2003). A 9 bp sequence encoding the peroxisomal targeting signal, SKL, was introduced upstream of the RFP stop codon. Both PCR fragment and vector pESC-TRP (Stratagene) were cut with *Spe*I/*Pac*I and ligated to generate plasmid pESC-RFP_{SKL}.

All plasmid constructs were verified by sequencing (MWG, Martinsried, Germany) (Table 3.1b).

3.2.3. Chromosomal integration of *pcbAB* and *npgA*

Three fragments were generated for integration at position YCRWdelta11 (Figure 3.2). Fragment 1 is the result of a fusion of two PCR products: the upstream flank of the integration site, which was amplified from genomic DNA using primer pair P4/Pxc024, and *npgA* including *GAL1* promoter and *CYC1* terminator, which was amplified from plasmid pESC-npgA-pcbAB using primers Pxc016 and Pxc017. Since a tail had been added to primer Pxc024, both PCR products shared an overlapping sequence that allowed them to fuse in an additional PCR using the outer primers for amplification. Accordingly, fragment 3 was produced through fusion PCR of three PCR products: the 3' region of *pcbAB* and the *ADH1* terminator amplified from pESC-npgA-pcbAB with primers Pxc018 and Pxc019, the *Kluyveromyces lactis URA3* locus with direct repeats amplified from vector pWJ1042 (Reid et al., 2002) using primer pair Pxc20/Pxc21, and the downstream flank of the integration site amplified with primers Pxc22 and Pxc23. Fragment 2 containing the bi-directional *GAL1*/*GAL10* promoter and the *pcbAB* gene was isolated from vector pESC-npgA-

pcbAB after restriction with *Xma*I/*Pac*I. Co-transformation of all three fragments enabled chromosomal integration by homologous recombination at four positions as indicated in Figure 3.2. Correct integration was confirmed by PCR and sequencing of the resulting PCR products. Subsequently, the cells were cultivated on plates containing 5-fluoroorotic acid (5-FOA). This led to the selection of clones that had lost the *K.l. URA3* marker via homologous recombination between the two flanking direct repeats.

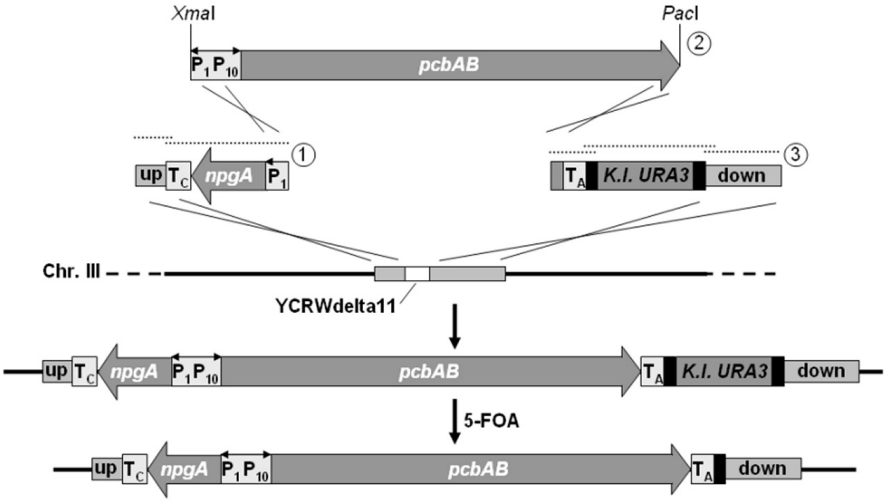

Figure 3.2. Chromosomal integration of *npgA* and *pcbAB*: direct repeats flanking *K.l. URA3* are indicated as black bars. P_1P_{10}, bi-directional *GAL1*/*GAL10* promoter; T_A, *ADH1* terminator; T_C, *CYC1* terminator; up, upstream flank; down, downstream flank and 5-FOA, 5-fluoroorotic acid. Dotted lines indicate primary PCR products, which were fused to generate fragments 1 and 2.

3.2.4. Fluorescence microscopy

Cells were harvested by centrifugation, washed in SG medium and mixed with an equal volume of 1.2% (w/v) low melting agarose (Cambrex, Rockland, ME, USA) on a microscope slide for immobilisation. In order to visualize DNA 10 µg/ml 4',6-diamidino-2-phenylindole (DAPI) (Sigma-Aldrich, St. Louis, MO, USA) was added to the cultures 30 min before harvesting. Live cell images were captured with a cooled mono-12-bit QImaging Retiga EXi camera mounted on a Nikon Eclipse E1000 microscope. All images were captured using a Nikon Plan Flour 100 x, 1.30

numerical aperture objective lens. The illumination source was a 12V 100W LL mercury lamp. Images were acquired using Image Pro Plus 5.1 software (Media Cybernetics, Bethesda, MD, USA).

3.2.5. LC-MS analysis of ACV formation

Yeast strains expressing ACVS and a PPTase were grown in shake flasks containing SG medium. 30 ml of culture were harvested at late exponential or early stationary growth phase by centrifugation and cells were re-dissolved in 1 ml methanol. Mechanical disruption of the cells was achieved using glass beads and a Savant FastPrep FP120 at speed 4 for 5×30 s. After centrifugation, the supernatant was run at 20 °C on HPLC (Agilent 1100)-MS (Micromass LCT) with Phenomenex Gemini 3u C6-Phenyl 110A 50×2 mm column (with 2 mm guard column). A linear gradient of H_2O (containing 20 mM formic acid) and methanol (containing 20 mM formic acid) was used. The gradient was changed from 0 % methanol to 100 % over 20 min and then maintained at 100 % methanol for 5 min before returning to starting conditions. The flow rate was 0.3 ml/min. Mass spectra were collected from *m/z* 100 to 900. As a standard, ACV (Sigma-Aldrich) dissolved in methanol was used.

To compare ACV formation in different strains or at different conditions the area of the ACV peak was normalized to OD_{600} of the culture at harvesting and the harvested culture volume.

3.3. Results

3.3.1. Expression of ACVS and PPTase in *S. cerevisiae*

The *P. chrysogenum* ACVS encoding gene *pcbAB* and the *A. nidulans* PPTase encoding gene *npgA* were cloned into the pESC-URA vector containing a bi-directional galactose-inducible *GAL1*/*GAL10* promoter. *S. cerevisiae* strain CEN.PK 119-9D was transformed with the resulting plasmid. Strains were grown in SG medium containing galactose as sole carbon source at 30 °C. Transformants harbouring pESC-npgA-pcbAB showed no significant differences in the growth rate

compared to the strains containing the empty pESC-URA plasmid and transcription of *pcbAB* and *npgA* was confirmed using the reverse transcription (RT)-PCR analysis (data not shown).

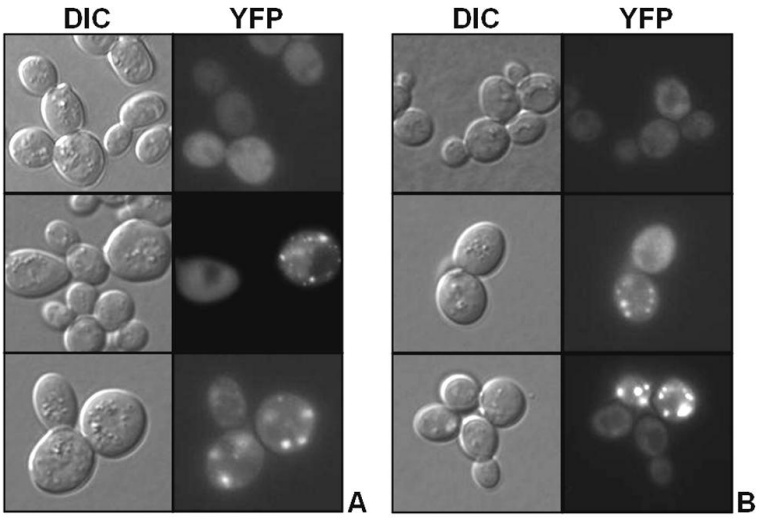

Figure 3.3. Fluorescence microscopy of yeast cells harboring plasmid pESC-npgA-pcbAB-YFP and cultivated in SG medium at 30 °C (A) and 20 °C (B). DIC, differential interference contrast.

To monitor expression of ACVS, yellow fluorescent protein (YFP) was fused to its C-terminus. After cultivation in SG medium at 30 °C, fluorescence was observed in strains harboring the pESC-npgA-pcbAB-YFP plasmid (Figure 3.3). However, the fluorescence signal was weak and not even visible in all of the examined cells suggesting a low expression level. Among these cells, two different expression patterns could be observed: dispersed fluorescence throughout the cytosol as well as fluorescent foci in some of the cells (Figure 3.3). ACVS has been reported to be located in the cytosol in *P. chrysogenum* (van der Lende et al., 2002). To verify that ACVS was localized in the cytosol in yeast and that the foci did not result from mistargeting, plasmid pESC-RFP_{SKL}, which allows expression of peroxisome-targeted red fluorescent protein (RFP), was co-expressed with pESC-npgA-pcbAB-YFP. In addition, mitochondrial DNA was stained with DAPI. Neither the peroxisomal nor the mitochondrial signal co-localized with the foci observed for YFP-tagged ACVS (data

not shown). Thus, ACVS appears to be located in the cytosol when expressed in *S. cerevisiae* and the observation of foci indicates the formation of protein aggregates.

3.3.2. Production of ACV in *S. cerevisiae*

Yeast strains harbouring ACVS and PPTase expression plasmid pESC-npgA-pcbAB were grown at 30 °C in shake flasks containing SG medium. As a negative control strains containing plasmid pESC-URA were cultivated under the same conditions. Methanol extracts from cells harvested at late exponential growth phase were analysed by LC-MS using pure ACV as a standard. ACV elutes at 6.6 min with a predominant ion at *m/z* 364.15, which corresponds to its protonated molecular ion. As shown in Figure 3.4, a peak with a similar *m/z* and retention time as the ACV standard was observed in the spectra from strains containing plasmid pESC-npgA-pcbAB, while no such peak was found in spectra from strains containing plasmid pESC-URA. The LC-MS results thus demonstrate the production of ACV in yeast strains expressing ACVS and PPTase.

When measuring the ACV content at different time points, we saw a decline during stationary phase (data not shown). Hence, all further cultivations for product detection were harvested in late exponential or early stationary phase.

For comparison of different strains and different conditions, ACV concentrations are given in arbitrary units in the following since the extraction method used in this study has not been thoroughly validated yet. However, assuming a 100% recovery, the measured ACV concentrations are in the range of 1µg - 1 mg/g dry cell weight.

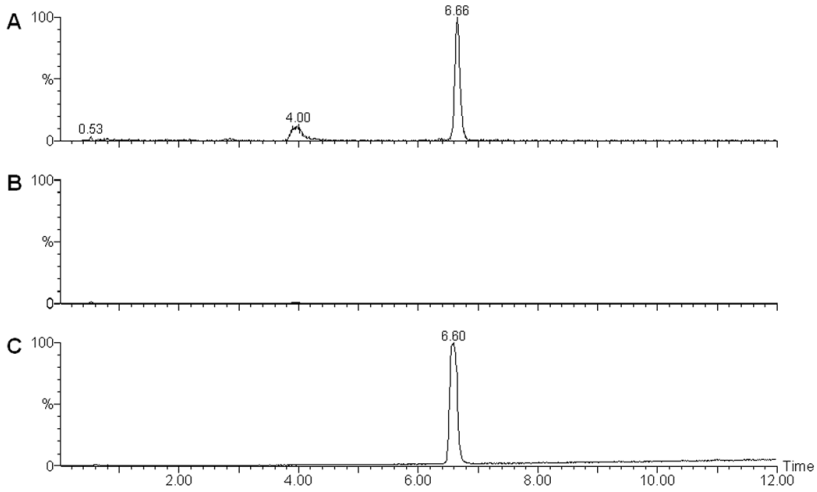

Figure 3.4. LC-MS analysis: ion traces for *m/z* 364.15 of metabolites extracted from a strain carrying the pESC-npgA-pcbAB plasmid (A), of metabolites extracted from a strain carrying the pESC-URA plasmid (B) and of the ACV standard (C).

3.3.3. Enhancement of ACV production in *S. cerevisiae*

The ACV concentrations measured in producing yeast strains were often close to the detection limit. Therefore, three approaches were followed to enhance ACV production in *S. cerevisiae*: (i) implementation of three different PPTases to ensure optimal transfer of the 4'-phosphopantetheine cofactor, (ii) codon optimization of the 5' end of *pcbAB* to increase the translation efficiency and (iii) lowering the cultivation temperature to improve protein folding.

In the first approach, two PPTases different from NpgA were expressed together with ACVS: PptA, the native activator of *P. chrysogenum* ACVS and Sfp, a broad specificity PPTase of *B. subtilis*. For this purpose, the *npgA* gene in plasmid pESC-npgA-pcbAB was replaced with *pptA* and *sfp*. Yeast harboring plasmids pESC-npgA-pcbAB, pESC-pptA-pcbAB and pESC-sfp-pcbAB were cultivated at 30 ºC and cell extracts were analysed by LC-MS. The results showed that implementation of different PPTases had no influence on the ACV production in yeast (Table 3.2a).

Codon optimization of the 5' end of the coding sequence can assist to improve the yield of a heterologously expressed protein (Batard et al., 2000; Johansson et al., 1999; Mutka et al., 2005). Since the 5' region of pcbAB contains a number of rare codons (codons used < 13 times per 1000 codons in the yeast genome; Carlini, 2005), 20 out of its first 27 codons were replaced by synonymous codons preferred in *S. cerevisiae*. Strains harboring plasmid pESC-optpcbAB and strains containing plasmid pESC-npgA-pcbAB were cultivated at 30 ºC. Cell extracts were analyzed by LC-MS. A slight increase in ACV production was observed, which was however not statistically significant (Table 3.2a).

Table 3.2a. ACV production of plasmid carrying strains at 30°C [a]

Plasmid	ACV (arbitrary units)	SD
pESC-npgA-pcbAB	40.8	28.5
pESC-pptA-pcbAB	40.7	18.5
pESC-sfp-pcbAB	48.8	16.9
pESC-optpcbAB	83.2	30.9

[a] ACV was measured in two to six independent cultures of each type of strain and experiments were at least performed twice.

The protein aggregates observed for YFP-tagged ACVS may represent the result of an improper folding process. Protein misfolding problems can often be compensated by growing cells at low temperature (Li et al., 2001; Weickert et al., 1997). To investigate the influence of low temperature cultivation on protein aggregation, yeast strains expressing ACVS-YFP were cultivated at 30 °C and 20 °C. Growth at 20 °C seemed to enhance the fluorescence intensity as observed under the microscope (not shown). However, the cells still contained ACVS-YFP aggregates indicated by the presence of fluorescent foci (Figure 3.3).

Even though low temperature cultivation did not prevent the formation of protein aggregates, it had a pronounced effect on the ACV production level. Cell extracts of strains carrying plasmid pESC-optpcbAB and grown at 30 °C, 20 °C and 15 °C were analyzed by LC-MS. Strains grown at 20 °C had a 30-fold higher ACV content than those cultivated at 30 °C while there was no further improvement in ACV production by lowering the cultivation temperature from 20 °C to 15 °C (Table 3.2b).

When the strains containing either the original or the codon optimised version of ACVS were cultivated at 20 °C, no significant differences in ACV production were observed (Table 3.2c). The same was true for the strains expressing either of the three different PPTases at low temperature cultivation (data not shown).

3.3.4. Chromosomal integration

In order to investigate the effect of gene dosage on ACV production in yeast, we constructed strains containing a single copy of the ACVS and PPTase encoding genes. *PcbAB* and *npgA* were integrated into the yeast genome (Figure 3.2). To reduce the possibility of affecting the expression of other genes a long terminal repeat (LTR), which marks the previous position of a retrotransposon, was chosen as the integration site in this study. The *GAL1*/*GAL10* promoter already used in the pESC-npgA-pcbAB construct was also used in the integrated strain, to obtain controlled gene expression.

The integrated strain as well as the plasmid containing strain harboring pESC-npgA-pcbAB, were cultivated at 20 ºC. The LC-MS results showed that ACV production in the integrated strain was about 6-fold lower than that observed in the plasmid carrying strain (Table 3.2d).

Table 3.2b. ACV production of pESC-optpcbAB containing strains [a]

Temperature (°C)	ACV (arbitrary units)	SD
30	255	61
20	9158	1148
15	7514	1846

[a] ACV was measured in two to six independent cultures of each type of strain and experiments were at least performed twice.

Table 3.2c. ACV production of plasmid carrying strains at 20°C [a]

Plasmid	ACV (arbitrary units)	SD
pESC-npgA-pcbAB	8004	1566
pESC-optpcbAB	9312	875

[a] ACV was measured in two to six independent cultures of each type of strain and experiments were at least performed twice.

Table 3.2d. ACV production of integrated vs. plasmid carrying strains at 20°C [a]

Strain	ACV (arbitrary units)	SD
plasmid harbouring	807.6	382.0
integrated	120.8	12.2

[a] ACV was measured in two to six independent cultures of each type of strain and experiments were at least performed twice.

3.4. Discussion

During the past decade *S. cerevisiae* has been established as a production host for a number of different metabolites with applications in the pharmaceutical or food industry (Huang et al., 2008). In the present study, we initiated the implementation of yeast for production of a versatile class of secondary metabolites — the non-ribosomal peptides. Using ACV synthetase as a model, we demonstrated the possibility of non-ribosomal peptide synthesis in yeast when the NRP synthetase is co-expressed with a Sfp-type PPTase. The two PPTases Sfp from *B. subtilis* and NpgA derived from *A. nidulans* have previously successfully been used for heterologous polyketide production in yeast (Kealey et al., 1998; Wattanachaisaereekul et al., 2007; Wattanachaisaereekul et. al., 2008). In our study, the choice of PPTase seems to be of less importance since ACV production levels using either NpgA, PptA or Sfp for ACVS activation were similar. This is consistent with the reported broad substrate specificity of Sfp-type PPTases (Mootz et al., 2001; Quadri et al. 1998b).

We pursued two different strategies to improve ACVS expression and thus ACV production in yeast, the first of them being codon optimization. It is well known that each organism has its own preferred codon usage, which is strongly correlated with the tRNA content and protein expression levels of individual genes in the organism (Ikemura, 1985; Percudani et al., 1997). Codon biases have been reported to influence foreign protein expression profoundly (Kane, 1995). Moreover, it is believed that especially the codon composition at the beginning of a coding sequence plays an important role in protein expression (Vervoort et al., 2000). Improved yields of heterologously expressed proteins were successfully achieved by codon optimization

of the 5' end of the coding sequence in *E. coli* (Johansson et al., 1999) and yeast (Batard et al., 2000; Mutka et al., 2005). Optimization of as few as the first 14 codons was reported to enhance the expression of G+C-rich genes (Mutka et al., 2005). By contrast, changing the first 27 codons of ACVS with regard to the yeast codon bias had no significant effect on ACV production. However, codon optimization of further regions of *pcbAB* with a high frequency of codons rarely used in yeast or even the complete gene may still be a promising tool to enhance the ACV production level.

In a second strategy, which is commonly used in heterologous protein production, we lowered the cultivation temperature of the ACVS expressing yeast strains. Expression of heterologous proteins in biological hosts often results in problems with improper folding (Dobson and Karplus, 1999), which may result in low yield or activity of the enzyme and hereby in a low production level of the desired product. These misfolding problems can often be reduced by growing cells at low temperature (Gidijala et al., 2008; Li et al., 2001; Weickert et al., 1997). Our results on fluorescence microscopy of cells expressing an ACVS-YFP fusion protein indicated possible folding problems during ACVS expression in yeast. As expected, fluorescence occurred in the cytosol, albeit partially in the form of foci indicating the formation of insoluble aggregates potentially as a result of an improper folding process. Reducing the cultivation temperature from 30 to 20 °C profoundly increased the ACV production level by a factor of 30 supporting the theory of improved protein folding conditions at low temperature. However, low cultivation temperature did not inhibit the formation of ACVS-YFP aggregates. Investigations on bacterial inclusion bodies have shown that heterologous proteins occurring in the form of aggregates may still be properly folded (Ventura and Villaverde, 2006) and that not only protein solubility is influenced by growth temperature, but also conformational quality of recombinant proteins, even in the insoluble fraction (Vera et al., 2007).

When integrating the ACVS and PPTase encoding genes into the chromosomal DNA another rate-limiting factor for ACV production in *S. cerevisiae* was detected – the gene copy number. Integrated strains produced 6 times less ACV than plasmid carrying strains. On the other hand, chromosomal integration bears the advantage of

higher mitotic stability in comparison to plasmid-based expression. Thus, multiple copy integration could be considered.

We noticed a relatively high variation in ACV production of the same strains in different experiments (see also Tables 3.2a-3.2d), probably due to even slight differences in experimental conditions, leaving room for further improvement strategies.

In general, the present study represents a basis for a further development of *S. cerevisiae* as a cell factory for production of NRPs that are difficult to produce with their natural hosts. As a eukaryote, yeast may in many cases be a better candidate for the synthesis of antibiotics than prokaryotic expression systems. The easy amenability of yeast for genetic manipulation will allow a fast construction of new NRPSs containing specific point mutations or exchanged domains for the development of new NRPs with new or improved properties and metabolic engineering can help to reach suitable production levels within a reasonable amount of time (Chemler and Koffas, 2008; Huang et al., 2008; Olano et al., 2008).

Acknowledgements

XC was financially supported by a scholarship obtained from the Technical University of Denmark.

We would like to thank Hanne Jakobsen for excellent technical assistance as well as Kristian Fog Nielsen and Jørn Smedsgaard for helpful discussions.

References

Batard, Y., Hehn, A., Nedelkina, S., Schalk, M., Pallett, K., Schaller, H., Werck-Reichhart, D., 2000. Increasing expression of P450 and P450-reductase proteins from monocots in heterologous systems. Arch. Biochem. Biophys. 379, 161-169.

Byford, M.F., Baldwin, J.E., Shiau, C.Y., Schofield, C.J., 1997. The mechanism of ACV Synthetase. Chem. Rev. 97, 2631-2650.

Carlini, D.B. 2005. Context-dependent codon bias and messenger RNA longevity in the yeast transcriptome. Mol. Biol. Evol. 22, 1403-1411.

Chemler, J.A., Koffas, M.A.G. 2008. Metabolic engineering for plant natural product biosynthesis in microbes. Curr. Opin. Biotechnol. 19, 597-605.

Dobson, C.M., Karplus, M., 1999. The fundamentals of protein folding: bringing together theory and experiment. Curr. Opin. Struct. Biol. 9, 92-101.

Ehmann, D.E., Gehring, A.M., Walsh, C.T., 1999. Lysine biosynthesis in *Saccharomyces cerevisiae*: mechanism of alpha-aminoadipate reductase (Lys2) involves posttranslational phosphopantetheinylation by Lys5. Biochemistry 38, 6171-6177.

Eppelmann, K., Doekel, S., Marahiel, M.A., 2001. Engineered biosynthesis of the peptide antibiotic bacitracin in the surrogate host *Bacillus subtilis*. J. Biol. Chem. 276, 34824-34831.

Fichtlscherer, F., Wellein, C., Mittag, M., Schweizer, E., 2000. A novel function of yeast fatty acid synthase. Subunit alpha is capable of self-pantetheinylation. Eur. J. Biochem. 267, 2666-2671.

Gidijala, L., Bovenberg, R.A.L., Klaassen, P., van der Klei, I.J., Veenhuis, M., Kiel, J.A.K.W., 2008. Production of functionally active *Penicillium chrysogenum* isopenicillin N synthase in the yeast *Hansenula polymorpha*. BMC Biotechnol. 8, 29.

Huang, B., Guo, J., Yi, B., Yu, X., Sun, L., Chen, W., 2008. Heterologous production of secondary metabolites as pharmaceuticals in *Saccharomyces cerevisiae*. Biotechnol. Lett. 30, 1121-1137.

Ikemura, T., 1985. Codon usage and tRNA content in unicellular and multicellular organisms. Mol. Biol. Evol. 2, 13-34.

Johansson, A.S., Bolton-Grob, R., Mannervik, B., 1999. Use of silent mutations in cDNA encoding human glutathione transferase M2-2 for optimized expression in *Escherichia coli*. Protein Expr. Purif. 17, 105-112.

Kane, J.F., 1995. Effects of rare codon clusters on high-level expression of heterologous proteins in *Escherichia coli*. Curr. Opin. Biotechnol. 6, 494-500.

Kealey, J.T., Liu, L., Santi, D.V., Betlach, M.C., Barr, P.J., 1998. Production of a polyketide natural product in nonpolyketide-producing prokaryotic and eukaryotic hosts. Proc. Natl. Acad. Sci. USA 95, 505-509.

Keszenman-Pereyra, D., Lawrence, S., Twfieg, M.E., Price, J., Turner, G., 2003. The *npgA*/ *cfwA* gene encodes a putative 4'-phosphopantetheinyl transferase which is essential for penicillin biosynthesis in *Aspergillus nidulans*. Curr. Genet. 43, 186-190.

Kleinkauf, H., von Doehren, H., 1996. A nonribosomal system of peptide biosynthesis. Eur. J. Biochem. 236, 335-351.

Lambalot, R.H., Gehring, A.M., Flugel, R.S., Zuber, P., LaCelle, M., Marahiel, M.A., Reid, R., Khosla, C., Walsh, C.T., 1996. A new enzyme superfamily - the phosphopantetheinyl transferases. Chem. Biol. 3, 923-936.

Li, Z., Xiong, F., Lin, Q., d'Anjou, M., Daugulis, A.J., Yang, D.S., Hew, C.L., 2001. Low-temperature increases the yield of biologically active herring antifreeze protein in *Pichia pastoris*. Protein Expr. Purif. 21, 438-445.

Lisby, M., Mortensen, U.H., Rothstein, R., 2003. Colocalization of multiple DNA double-strand breaks at a single Rad52 repair centre. Nat. Cell Biol. 5, 572-577.

Molnar, I., Schupp, T., Ono, M., Zirkle, R.E., Milnamow, M., Nowak-Thompson, B., Engel, N., Toupet, C., Stratmann, A., Cyr, D.D., Gorlach, J., Mayo, J.M., Hu, A., Goff, S., Schmid, J., Ligon, J.M., 2000. The biosynthetic gene cluster for the microtubule-stabilizing agents epothilones A and B from *Sorangium cellulosum* So ce90. Chem. Biol. 7, 97-109.

Mootz, H.D., Finking, R., Marahiel, M.A., 2001. 4'-Phosphopantetheine transfer in primary and secondary metabolism of *Bacillus subtilis*. J. Biol. Chem. 276, 37289-37298.

Mutka, S.C., Bondi, S.M., Carney, J.R., Da Silva, N.A., Kealey, J.T., 2005. Metabolic pathway engineering for complex polyketide biosynthesis in *Saccharomyces cerevisiae*. FEMS Yeast Res. 6, 40-47.

Olano, C., Lombó, F., Méndez, C., Salas, J.A. 2008. Improving production of bioactive secondary metabolites in actinomycetes by metabolic engineering. Metab. Eng. 10, 281-292.

Percudani, R., Pavesi, A., Ottonello, S., 1997. Transfer RNA gene redundancy and translational selection in *Saccharomyces cerevisiae*. J. Mol. Biol. 268, 322-330.

Quadri, L.E., Sello, J., Keating, T.A., Weinreb, P.H., Walsh, C.T., 1998a. Identification of a *Mycobacterium tuberculosis* gene cluster encoding the biosynthetic enzymes for assembly of the virulence-conferring siderophore mycobactin. Chem. Biol. 5, 631-645.

Quadri, L.E., Weinreb, P.H., Lei, M., Nakano, M.M., Zuber, P., Walsh, C.T., 1998b. Characterization of Sfp, a *Bacillus subtilis* phosphopantetheinyl transferase for peptidyl carrier protein domains in peptide synthetases. Biochemistry 37, 1585-1595.

Reid, R., Lisby, M., Rothstein, R., 2002. Cloning-free genome alterations in *Saccharomyces cerevisiae* using adaptamer-mediated PCR. Methods Enzymol. 350, 258-77.

Schoergendorfer, K., Kurnsteiner, H., 2005. New isolated *Penicillium chrysogenum* 4'-phosphopantethein transferase PPTase protein, useful for producing penicillin G or penicillin V. Patent WO2005040369.

Schwarzer, D., Finking, R., Marahiel, M.A., 2003. Nonribosomal peptides: from genes to products. Nat. Prod. Rep. 20, 275-287.

Sieber, S.A., Marahiel, M.A., 2005. Molecular mechanisms underlying nonribosomal peptide synthesis: approaches to new antibiotics. Chem. Rev. 105, 715-738.

Smith, D.J., Earl, A.J., Turner, G., 1990. The multifunctional peptide synthetase performing the first step of penicillin biosynthesis in *Penicillium chrysogenum* is a 421,073 dalton protein similar to *Bacillus brevis* peptide antibiotic synthetases. EMBO J. 9, 2743-2750.

van der Lende, T.R., van de Kamp, M., van den Berg, M., Sjollema, K., Bovenberg, R.A.L., Veenhuis, M., Konings, W.N., Driessen, A.J.M., 2002. δ-(L-α-

Aminoadipyl)-L-cysteinyl-D-valine synthetase, that mediates the first committed step in penicillin biosynthesis, is a cytosolic enzyme. Fungal Genet. Biol. 37, 49-55.

van Wageningen, A.M., Kirkpatrick, P.N., Williams, D.H., Harris, B.R., Kershaw, J.K., Lennard, N.J., Jones, M., Jones, S.J., Solenberg, P.J., 1998. Sequencing and analysis of genes involved in the biosynthesis of a vancomycin group antibiotic. Chem. Biol. 5, 155-162.

Ventura, S., Villaverde, A., 2006. Protein quality in bacterial inclusion bodies. Trends Biotechnol. 24, 179-185.

Vera, A., González-Montalbán, N., Arís, A., Villaverde, A., 2007. The conformational quality of insoluble recombinant proteins is enhanced at low growth temperatures. Biotechnol. Bioeng. 96, 1101-1106.

Vervoort, E.B., van Ravestein, A., van Peij, N.N.M.E., Heikoop, J.C., van Haastert, P.J.M., Verheijden, G.F., Linskens, M.H.K., 2000. Optimizing heterologous expression in *Dictyostelium*: importance of 5' codon adaptation. Nucleic Acids Res. 28, 2069-2074.

Wattanachaisaereekul, S., Lantz, A.E., Nielsen, M.L., Andrésson, O.S., Nielsen, J., 2007. Optimization of heterologous production of the polyketide 6-MSA in *Saccharomyces cerevisiae*. Biotechnol. Bioeng. 97, 893-900.

Wattanachaisaereekul, S., Lantz, A.E., Nielsen, M.L., Nielsen, J., 2008. Production of the polyketide 6-MSA in yeast engineered for increased malonyl-CoA supply. Metab. Eng. 10, 246-254.

Weber, G., Leitner, E., 1994. Disruption of the cyclosporin synthetase gene of *Tolypocladium niveum*. Curr. Genet. 26, 461-467.

Weickert, M.J., Pagratis, M., Curry, S.R., Blackmore, R., 1997. Stabilization of apoglobin by low temperature increases yield of soluble recombinant hemoglobin in *Escherichia coli*. Appl. Environ. Microbiol. 63, 4313-4320.

Chapter 4. Increased isobutanol production in *Saccharomyces cerevisiae* by overexpression of genes in valine metabolism

Xiao Chen*, Kristian Fog Nielsen, Irina Borodina, Morten C. Kielland-Brandt, Kaisa Karhumaa

Submitted to ***Biotechnology for Biofuels***

Abstract

Background

Isobutanol can be a better biofuel than ethanol due to its higher energy density and lower hygroscopicity. Furthermore, the branched-chain structure of isobutanol gives a higher octane number than the isomeric *n*-butanol. *Saccharomyces cerevisiae* was chosen as the production host because of its relative tolerance to alcohols, robustness in industrial fermentations, and the possibility for future combination of isobutanol production with fermentation of lignocellulosic materials.

Results

The yield of isobutanol was improved from 0.16 to 0.97 mg per g glucose by simultaneous overexpression of biosynthetic genes *ILV2*, *ILV3*, and *ILV5* in valine metabolism in anaerobic fermentation of glucose in mineral medium in *S. cerevisiae*. Isobutanol yield was further improved by two times by the additional overexpression of *BAT2*, encoding the cytoplasmic branched-chain amino acid aminotransferase. Overexpression of *ILV6,* encoding the regulatory subunit of Ilv2, in the *ILV2 ILV3 ILV5* overexpression strain decreased isobutanol production yield by three times. In aerobic cultivations in shake flasks in mineral medium, the isobutanol yield of the *ILV2 ILV3 ILV5* overexpression strain and the reference strain were 3.86 and 0.28 mg per g glucose, respectively. They were increased to 4.12 and 2.4 mg per g glucose in YPD complex medium under aerobic conditions, respectively.

Conclusions

Overexpression of genes *ILV2*, *ILV3*, *ILV5*, and *BAT2* in valine metabolism led to an increase in isobutanol production in *S. cerevisiae*. Additional overexpression of *ILV6* in the *ILV2 ILV3 ILV5* overexpression strain had a negative effect, presumably by increasing the sensitivity of Ilv2 to valine inhibition, thus weakening the positive impact of overexpression of *ILV2*, *ILV3*, and *ILV5* on isobutanol production.

Aerobic cultivations of the *ILV2 ILV3 ILV5* overexpression strain and the reference strain showed that supplying amino acids in cultivation media gave a substantial improvement in isobutanol production for the reference strain, but not for the *ILV2 ILV3 ILV5* overexpression strain. This result implies that other constraints besides the enzyme activities for the supply of 2-ketoisovalerate may become bottlenecks for isobutanol production after *ILV2*, *ILV3*, and *ILV5* have been overexpressed, which most probably include the valine inhibition to Ilv2.

4.1. Background

Environmentally friendly production of biofuels is a target of great interest due to climate change and the need for renewable transportation fuels. Microbial production of chemicals to be used as liquid biofuels will allow the use of renewable raw materials such as lignocellulose. Optimally, biomass from agricultural and forestry waste products could be used as raw material.

Bioethanol is the most established biofuel, with existing commercial production. Several pilot plants are in operation for lignocellulosic ethanol production in several countries. However, the chemical properties of ethanol, such as high tendency to absorb water, are not optimal for all purposes. For many purposes, such as jet fuel, better properties are required with regard to hygroscopicity and energy density. Higher alcohols, such as *n*-butanol and isobutanol, represent possible alternatives. Compared with *n*-butanol, isobutanol has the advantage of having a higher octane number, and the possibility of usage also outside the fuel industry [1].

Microbial production of isobutanol has been studied in food fermentations and alcoholic beverages for flavor profiling since the 1970s [2, 3]. In recent years, production of isobutanol was investigated as a biofuel in engineered *Escherichia coli* to reach a concentration of 22 g/L during aerobic cultivations [4]. However, as isobutanol concentrations over 15 g/L are toxic to *E. coli* [5], this concentration may also be close to the maximal possible production in this bacterium. Since *Corynebacterium glutamicum* is more tolerant to isobutanol than is *E. coli*, it was engineered as a host and produced about 4 g/L of isobutanol in the presence of oxygen [5]. Yeast is well known to be tolerant to alcohols. *Saccharomyces cerevisiae* is tolerant to up to 20% ethanol [6]. In a test of many microbial strains for butanol tolerance, baker's yeast *S. cerevisiae* and *Lactobacilli* were the only microbes able to grow in butanol concentrations higher than 20 g/l [7]. In addition, yeast is relatively robust in other respects, commonly used in fermentations with harsh conditions, and its outstanding performance in lignocellulosic hydrolysates would enable future combination of the higher alcohol production with fermentation of lignocellulosic materials. Yeast naturally produces small amounts of higher alcohols through the degradation of amino acids [8, 9], such as isobutanol among others [2, 3]. These are of great importance in the flavor profiles of beer and wine, as they generate desired fruity aromas to these products when produced in favorable amounts. Use of a host that naturally produces isobutanol may in principle offer an opportunity to avoid the use of heterologous pathways, which often require extensive work for optimal expression. According to all these advantages, *S. cerevisiae* is a potential alternative host for higher alcohol production.

We studied the effect of concomitant overexpression of several structural genes from the endogenous yeast valine biosynthetic pathway (Figure 4.1) for anaerobic isobutanol production in *S. cerevisiae*. It is well studied how yeast can convert valine to isobutanol [9], in other words isobutanol is a side product of valine synthesis, and our interest was whether increased flux in the valine biosynthetic pathway would increase isobutanol production. Isobutanol can be produced from pyruvate via formation of 2-ketoisovalerate (Figure 4.1). First, acetolactate synthase (Ilv2+Ilv6) converts 2 molecules of pyruvate to 2-acetolactate, which is then reduced to 2,3-dihydroxy-isovalerate by acetohydroxyacid reductoisomerase (Ilv5). Further, 2,3-

dihydroxy-isovalerate is converted to 2-ketoisovalerate by dihydroxyacid dehydratase (Ilv3). Ilv6 is the regulatory subunit of acetolactate synthase and an enhancer of Ilv2 catalytic activity. The bidirectional reaction between 2-ketoisovalerate and valine is catalyzed by the branched-chain amino acid aminotransferases (Bat1 and Bat2, present in the mitochondrial matrix and the cytosol, respectively). At last the 2-ketoisovalerate is converted to isobutanol by pyruvate decarboxylases (PDC) and alcohol dehydrogenases (ADH). We have here used overexpression of the valine pathway genes *ILV2*, *ILV3*, and *ILV5* to generate a 6-fold higher isobutanol yield. The finding that the isobutanol production in yeast that ferments a rich, complex medium could be increased by overexpression of Bat2 [10] prompted us to overexpress *BAT2* additional to the overexpression of *ILV2*, *ILV3*, and *ILV5* in synthetic medium. This turned out to increase isobutanol production further by two fold. However, overexpression of *ILV6*, encoding the regulatory subunit of the first committed step in valine biosynthesis, weakened the impact of overexpression of *ILV2*, *ILV3*, and *ILV5* on isobutanol production. After the initiation of the present work, results of somewhat similar genetic approaches on isobutanol production in *S. cerevisiae* appeared in patent applications [11, 12], but not in the refereed scientific literatures.

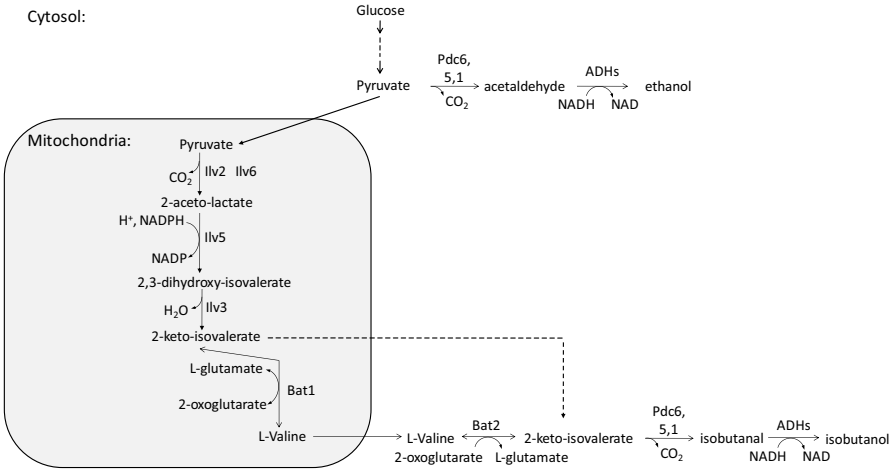

Figure 4.1. The metabolic pathways from pyruvate to isobutanol and ethanol in *S. cerevisiae*. The enzymes that catalyze the pathway from pyruvate to L-valine in the mitochondria are: acetolactate synthase (Ilv2+Ilv6), acetohydroxyacid reductoisomerase (Ilv5), dihydroxyacid dehydratase (Ilv3), and branched-chain amino acid aminotransferase (Bat1). Ilv2 is the catalytic subunit of acetolactate synthase, and Ilv6 is the regulatory subunit. The enzymes that catalyze the pathway from L-valine to isobutanol in the cytosol are pyruvate decarboxylases (Pdc6, 5, 1) and alcohol dehydrogenases (ADHs). Pyruvate decarboxylases and alcohol dehydrogenases also catalyze the pathway from pyruvate to ethanol in *S. cerevisiae*. The broken line indicates the export of 2-keto-isovalerate from mitochondria to cytosol.

4.2. Results and discussion

The objective of this work was to study isobutanol formation in *S. cerevisiae*, and to improve isobutanol production by metabolic engineering. We studied overexpression of the genes *ILV2*, *ILV3*, *ILV5*, *ILV6*, and *BAT2*, involved in valine metabolism, in different combinations, and investigated the isobutanol production in the constructed strains.

4.2.1. Improvement of anaerobic isobutanol production by overexpression of genes in valine metabolism

To overexpress the genes, *ILV2*, *ILV3*, and *ILV5*, which encode the catalysts for the conversion of pyruvate to 2-keto-isovalerate (direct precursor of L-valine), the coding regions were fused with the *S. cerevisiae PGK1* promoter. The resulting PGK1-ILV2, PGK1-ILV3 and PGK1-ILV5 DNA fusion fragments were cloned into integration vectors YDp-L, YDp-W, and YDp-H [13], respectively. The three resulting plasmids were linearized by cleavage of the *ILV* genes and successively integrated into the genome of CEN.PK 2-1C (*MATα leu2-3, 112 his3-Δ1 ura3-52 trp1-289 MAL2-8*(Con) *MAL3 SUC3*) (a kind gift of Peter Kötter, Frankfurt, Germany). The resulting strain was designated ILV235_XCY561 (*ILV2 ILV3 ILV5* overexpression strain). Successful genomic integration was confirmed by analytical PCR on chromosomal DNA. The copy number of the integrated gene was estimated by performing quantitative real-time PCR with genomic DNA as template [14, 15]. The estimates of the copy numbers of *ILV2*, *ILV3*, and *ILV5* in ILV235_XCY561 given by the quantitative PCR were 4.1±0.90, 2.1±0.65, and 3.6±1.12 times larger than those in the reference strain, respectively. Multiple integrations might happen in some cases. The expression of *ILV2*, *ILV3*, and *ILV5* at the transcriptional level in ILV235_XCY561 was also measured by quantitative real-time PCR. The mRNA levels of *ILV2*, *ILV3*, and *ILV5* in ILV235_XCY561 measured by qPCR were 6.42±2.20, 9.98±1.31, and 3.24±0.61 times larger than those in the reference strain, respectively. Overexpression of these three genes at mRNA level was proved. However, no enzymatic assays were performed to confirm the overexpression since the reagents needed are not commercially available.

The *ILV2 ILV3 ILV5* overexpressing strain (ILV235_XCY561) and the reference strain (CEN.PK 113-5D) were cultivated in mineral glucose medium supplemented with uracil in fermenters under anaerobic conditions. Primary metabolite concentrations were measured by high-performance liquid chromatography (HPLC) throughout the fermentation. Isobutanol concentration was measured by gas chromatography (GC) only from the samples taken at the end of fermentations after glucose depletion, due to the large sample volume needed for reliable measurements. The *ILV2 ILV3 ILV5* overexpression strain produced 0.97±0.14 mg isobutanol per g glucose, which was 6 times more than the reference strain (Figure 4.2). No difference was detected between the *ILV2 ILV3 ILV5* overexpression strain and the reference strain in the production of biomass, ethanol, pyruvate, succinate, glycerol, acetate and CO_2 (Table 4.1). Our interpretation is that overexpression of gene *ILV2*, *ILV3*, and *ILV5* led to a higher concentration of 2-keto-isovalerate, which resulted in higher isobutanol production.

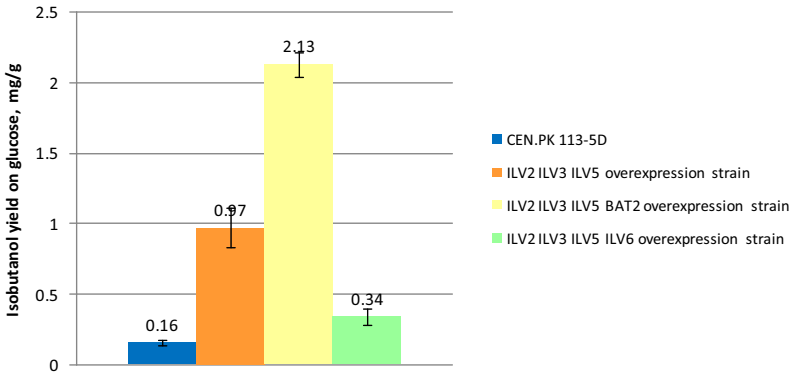

Figure 4.2. Effects of overexpression of *ILV* genes on isobutanol yield under anaerobic conditions. Isobutanol yields (mg per g glucose) of the reference strain (CEN.PK 113-5D) and *ILV2 ILV3 ILV5*, *ILV2 ILV3 ILV5 BAT2*, *ILV2 ILV3 ILV5 ILV6* overexpression strains were presented with columns with different colors, and the values are shown on the tops of each column. All cultivations were carried out in fermenters in mineral medium with 40 g glucose per liter under anaerobic conditions.

The *ILV2 ILV3 ILV5* overexpression strain had a maximum specific growth rate of 0.29±0.02 hr^{-1}, which was slower than the maximum specific growth rate of the reference strain, which was 0.38±0.02 hr^{-1}. The slower growth rate may be due to a metabolic imbalance caused by the overexpression of the *ILV* genes, which affects some amino acids pools, or due to insufficient expression of the selection markers, which were put at different loci and might not work with the same efficiency as at their wild type locations.

BAT2 encodes a branched-chain amino acid aminotransferase, which catalyzes the first reaction in the catabolism of valine in the cytosol [16]. *BAT2* is highly expressed during stationary phase and repressed during logarithmic growth, which is the opposite way of the regulation of the mitochondrial branched-chain amino acid aminotransferase, encoded by *BAT1* [17]. It has been previously shown that overexpression of *BAT2* alone increases isobutanol concentration in wine fermentations [18]. We therefore decided to investigate whether overexpression of *BAT2* could complement the valine pathway overexpression and result in higher yields and concentrations of isobutanol.

An *ILV2 ILV3 ILV5 BAT2* overexpression strain, ILV235BAT2_XCY715, was thus constructed by using the same promoter and the same molecular strategy. The estimate of the copy number of gene *BAT2* in ILV235BAT2_XCY715 was 1.5±0.50 times larger than the one in the reference strain, which was in accordance with the expected copy number of two. The overexpression of *BAT2* at the transcriptional level in ILV235BAT2_XCY715 was 90.82±0.45 times larger than that in the reference strain. The different overexpression levels among *ILV2*, *ILV3*, *ILV5*, and *BAT2*, reflect the fact that the expression level controlled by inserted promoters depends on the surrounding sequence. Anaerobic fermentations with ILV235BAT2_XCY715 were carried out in fermenters under the conditions described above. The GC results showed that the *ILV2 ILV3 ILV5 BAT2* overexpression strain produced 13 times more isobutanol per gram of glucose than the reference strain, which is an improvement by two fold over that of the *ILV2 ILV3 ILV5* overexpression strain (Figure 4.2). The biomass yield on glucose of the *ILV2 ILV3 ILV5 BAT2* overexpression strain was 0.07±0.01 g per g glucose, which was lower than the biomass yields of the *ILV2 ILV3*

ILV5 overexpression strain and the reference strain, which were 0.10±0.00 and 0.11±0.01, respectively. Carbon balance calculation showed that after accounting for carbon in produced biomass, isobutanol, ethanol, pyruvate, succinate, glycerol, acetate, and CO_2, there was about 11 % carbon missing (Table 4.1). We have investigated whether the missing carbon could be explained by the increase in the production of 3-methyl butanol and 2-methyl butanol, since the *BAT2* encoding aminotransferase also catalyzes the first step in the leucine and isoleucine catabolisms, which produce 3-methyl butanol and 2-methyl butanol, respectively [9, 19, 20]. GC analysis showed that the yield of 3-methyl butanol increased from 0.28 to 0.48 mg per g glucose (0.0330% carbon) compared to the reference strain, and there was no increase observed in 2-methyl butanol yield. These increases, however, were not large enough to explain the missing carbon. The deviation in carbon balance could be due to some other products not included in the present analysis. The time profiles of anaerobic fermentations of the *ILV2 ILV3 ILV5 BAT2* overexpression strain and the CEN.PK 113-5D reference strain are presented in Figure 4.3 A and B, respectively. Glucose consumption and all measured production rates were much higher in the reference strain than in the *ILV2 ILV3 ILV5 BAT2* overexpression strain. The maximum specific growth rate of the *ILV2 ILV3 ILV5 BAT2* overexpression strain was 0.16±0.01 hr^{-1}, and thus much lower than that of the reference strain and the *ILV2 ILV3 ILV5* overexpression strain, which has the growth rate at 0.38±0.02 and 0.29±0.02 hr^{-1}, respectively. The decrease in growth rate could be due to the same reasons as explained earlier for the slow growth rate of the *ILV2 ILV3 ILV5* overexpression strain. The very high overexpression of *BAT2* might result in a further metabolic imbalance of some amino acids pools, and could be the cause the further drop of the growth rate of the *ILV2 ILV3 ILV5 BAT2* overexpression strain. An independent transformant of the *ILV2 ILV3 ILV5* overexpression strain with the *BAT2* overexpression construct, named ILV235BAT2_XCY723, was investigated, and it behaved identically to ILV235BAT2_XCY715.

Table 4.1. Effects of gene overexpression on growth rates and product yields under anaerobic batch fermentations[a]

Strain	Reference strain[b]	*ILV2 ILV3 ILV5* overexpression strain[b]	*ILV2 ILV3 ILV5 BAT2* overexpression strain[b]	*ILV2 ILV3 ILV5 ILV6* overexpression strain[b]
Specific growth rate, hr^{-1}	0.38 ± 0.02	0.29 ± 0.02	0.16 ± 0.01	0.18 ± 0.00
Biomass ($CH_{1.78}O_{0.6}N_{0.19}$) yield, g/g glucose	0.10 ± 0.00	0.11 ± 0.01	0.07 ± 0.01	0.11 ± 0.00
Ethanol yield, g/g glucose	0.38 ± 0.01	0.37 ± 0.02	0.34 ± 0.01	0.37 ± 0.00
Pyruvate yield, g/g glucose	0.0011 ± 0.007	0.0016 ± 0.0007	0.0032 ± 0.0006	0.0028 ± 0.0001
Succinate yield, g/g glucose	0.0016 ± 0.0006	0.0006 ± 0.0001	0.0028 ± 0.0001	0.0035 ± 0.0003
Glycerol yield, g/g glucose	0.100 ± 0.008	0.087 ± 0.006	0.095 ± 0.001	0.099 ± 0.003
Acetate yield, g/g glucose	0.0076 ± 0.0014	0.0088 ± 0.0010	0.0110 ± 0.0006	0.0069 ± 0.0003
CO_2 yield, g/g glucose	0.32 ± 0.01	0.39 ± 0.01	0.37 ± 0.04	0.41 ± 0.03
Carbon balance deviation, %[b]	5.9 ± 2.2	3.0 ± 4.0	10.9 ± 1.7	1.3 ± 1.7

[a] The mineral medium with 40 g per liter of glucose was used.

[b]The reference strain used was CEN.PK 113-5D; The *ILV2 ILV3 ILV5* overexpression strain used was ILV235_XCY561; The *ILV2 ILV3 ILV5 BAT2* overexpression strain used were ILV235BAT2_XCY715 and ILV235BAT2_XCY723; The *ILV2 ILV3 ILV5 ILV6* overexpression strain used was ILV2356_XCY605.

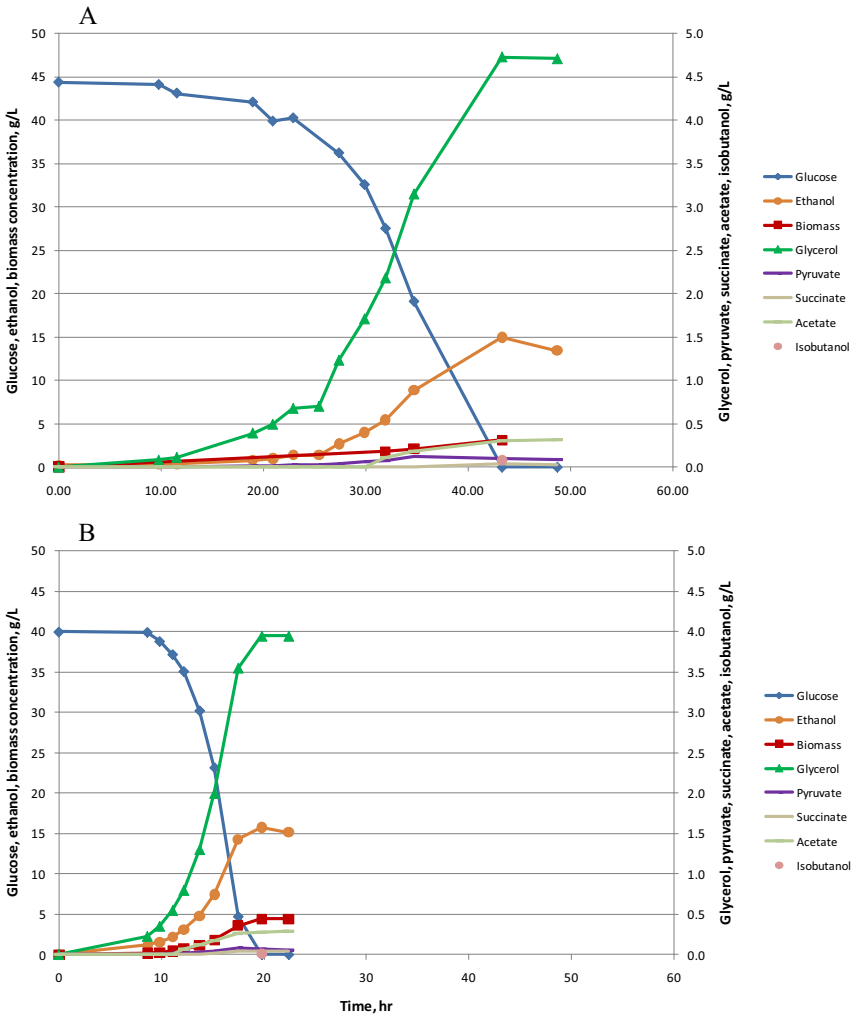

Figure 4.3. Time profiles of fermentations of *ILV2 ILV3 ILV5 BAT2* overexpression (A) and reference strain (B).
The *ILV2 ILV3 ILV5 BAT2* overexpression strain and the reference strain CEN.PK 113-5D were cultivated under anaerobic batch fermentations in mineral medium with 40 g glucose per liter. The concentrations of glucose, biomass, and products are plotted as a function of time. Isobutanol concentrations were measured after glucose depletion in both cases. Fermentations were performed in triplicate, representative cultivations are shown.

Ilv6 is the regulatory subunit of acetolactate synthase and has been described as an enhancer of Ilv2 catalytic activity. To investigate whether *ILV6* overexpression would further improve isobutanol production by possibly approaching equimolar amounts of both proteins, *ILV6* was overexpressed in the strain background with *ILV2*, *ILV3*, and *ILV5* overexpression. The resulting strain was designated ILV2356_XCY605, here

also referred to as the *ILV2 ILV3 ILV5 ILV6* overexpression strain. The estimate of the copy number of *ILV6* in ILV2356_XCY605 was 2.8±1.67 times larger than that in the reference strain. We also estimated the copy number of *ILV6* in ILV235BAT2_XCY715 and that of *BAT2* in ILV2356_XCY605. Their copy numbers were 0.9±0.31 and 1.0±0.42 times, respectively, compared to the reference strain, which was in agreement with the fact that these two genes were not overexpressed in their respective strains. The overexpression of *ILV6* at the transcriptional level in ILV2356_XCY605 was 8.07±1.14 times larger than that in the reference strain. Unexpectedly, integration of the overexpression construct with *ILV6* overexpression caused 3 times less isobutanol production, namely 0.34 mg per g glucose (Figure 4.2), and a drop of the maximum specific growth rate to 0.18±0.00 hr^{-1}. The yields of the other measured products, i.e. biomass, ethanol, pyruvate, succinate, glycerol, acetate, and CO_2 were largely unaffected (Table 4.1). We interpret the lower yield of isobutanol upon overexpression of *ILV6* to be due to an increased sensitivity of Ilv2 to valine inhibition, weakening the positive impact of overexpression of *ILV2*, *ILV3*, and *ILV5* on increasing isobutanol production in *S. cerevisiae*, since Ilv6 stimulates Ilv2 catalytic activity seven- to ten fold and confers Ilv2 sensitivity to valine inhibition [21, 22].

4.2.2. Influence of various media on isobutanol production and growth rate

The *ILV2 ILV3 ILV5* overexpression strain and the CEN.PK 113-5D reference strain were cultivated under aerobic conditions in shake flasks to further investigate the effect of valine pathway overexpression on growth rates and isobutanol production. Buffered mineral medium with 40 g glucose per liter and Yeast-extract Peptone Dextrose (YPD) complex medium with 17 g glucose per liter were used. The growth rates and the main product yields are shown in Table 4.2. In the mineral medium, the *ILV2 ILV3 ILV5* overexpression strain had a three times lower maximum specific growth rate (0.110 hr^{-1}) than the reference strain (0.359 hr^{-1}). In YPD, however, they grew at similar growth rates, about 0.5 hr^{-1}. Our interpretation is that genetic manipulations in the *ILV2 ILV3 ILV5* overexpression strain might cause a metabolic imbalance, which perhaps affected some amino acid pools, or the improper

functioning of the selection markers. Any of these problems could be compensated by growing the overexpression strain in the complex medium.

Isobutanol yields of the *ILV2 ILV3 ILV5* overexpression strain and the reference strain under aerobic cultivation conditions in different media are compared in Figure 4.4. In mineral medium the *ILV2 ILV3 ILV5* overexpression strain produced 3.86 mg isobutanol per g glucose, and the reference strain produced 0.28 mg isobutanol per g glucose. In YPD complex medium the *ILV2 ILV3 ILV5* overexpression strain and the reference strain produced 4.12 and 2.4 mg isobutanol per g glucose, respectively. There were 2.12 mg isobutanol per g glucose of increase for the reference strain, and only 0.26 mg isobutanol per g glucose of increase for the *ILV2 ILV3 ILV5* overexpression strain. We interpret this to be due to overexpression of *ILV2*, *ILV3*, and *ILV5* and uptake of valine from the complex medium both caused a strong increase of the pool of valine, and thereby an increase of isobutanol production. Since the provision of valine in the medium by using the YPD complex medium did not increase the isobutanol production yield of the *ILV2 ILV3 ILV5* overexpression strain much, it appears that other constraints besides the enzyme activities for the supply of 2-ketoisovalerate in the *ILV2 ILV3 ILV5* overexpression strain might have become bottlenecks. These could include valine inhibition to Ilv2, transportation of 2-ketoisovalerate or valine from mitochondria to cytosol, and affinities of PDCs to 2-ketoisovalerate in cytosol.

In this study, the isobutanol production yield was increased first by simultaneously overexpression genes, *ILV2*, *ILV3* and *ILV5* in valine biosynthetic pathway. However, which gene(s) out of these three is (are) needed to reach the same increased level of isobutanol yield, was not investigated in this study. Even though the isobutanol production yield was improved with 9 folds by overexpression of *ILV2*, *ILV3*, *ILV5*, and *BAT2*, in valine biosynthetic and degradation pathways, the isobutanol production yield was still too low for commercial applications. The low production of isobutanol was probably due to the regulation control of valine production in mitochodria, which limited the flux toisobutanol. Moving the pathway from pyruvate to 2-keto-isovalerate from mitochondria to cytosol would benefit the production of isobutanol in yeast.

Table 4.2. Aerobic batch cultivations of *ILV2 ILV3 ILV5* overexpression strain and reference strain in shake flasks[a]

Medium	Buffered mineral medium		YPD complex medium	
Strain	Reference stain[b]	*ILV2 ILV3 ILV5* overexpression strain[b]	Reference strain	*ILV2 ILV3 ILV5* overexpression strain
Specific growth rate, hr^{-1}	0.36± 0.00	0.11± 0.00	0.52± 0.00	0.50± 0.00
Biomass ($CH_{1.78}O_{0.6}N_{0.19}$) yield, g/g glucose	0.33± 0.06	0.14± 0.05	0.34± 0.00	0.35± 0.00
Ethanol yield, g/g glucose	0.22± 0.05	0.28± 0.10	0.12± 0.01	0.19± 0.02
Pyruvate yield, g/g glucose	0.0002±0.0000	0.0002± 0.0000	0.0137± 0.0003	0.0134± 0.0005
Succinate yield, g/g glucose	0.20± 0.02	0.26± 0.01	0.02± 0.00	0.01± 0.00
Glycerol yield, g/g glucose	0.006± 0.006	0.026± 0.017	0.002± 0.000	0.013± 0.000
Acetate yield, g/g glucose	0.0000±0.0000	0.0052± 0.0022	0.0929± 0.0047	0.0929± 0.0018

[a] The cultivations were carried out in shake flask. Buffered mineral medium containing 40 g/L glucose and YPD complex medium containing 17 g/L glucose were used.

[b] The reference strain used was CEN.PK 113-5D. The overexpression strain used was ILV235_XCY561.

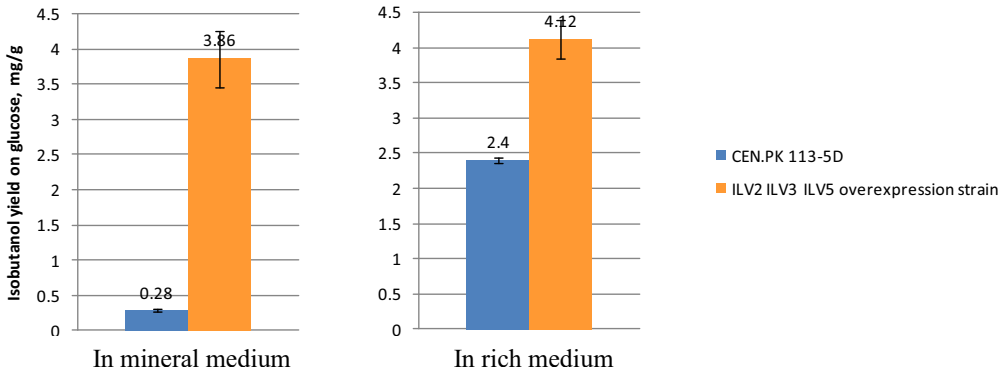

Figure 4.4. Effects of gene overexpression on isobutanol yield in various media under aerobic conditions.
The isobutanol yields (mg per g glucose) of the reference strain (CEN.PK 113-5D) and *ILV2 ILV3 ILV5* overexpression strains are presented with columns with different colors, and the values are shown on the top of each column. All cultivations were carried out aerobically in shake flasks in either mineral medium with 40 g glucose per liter or YPD complex medium with 17 g glucose per liter.

4.3. Conclusions

Isobutanol production yield on glucose was first increased from 0.16 to 0.97 mg isobutanol per gram of glucose by overexpression of genes *ILV2*, *ILV3*, and *ILV5*, which encode the catalysts for the conversion of pyruvate to 2-keto-isovalerate, the immediate precursor of valine. With the background of *ILV2 ILV3 ILV5* overexpression, isobutanol yield was further improved two-fold by overexpression of *BAT2*, encoding the catalyst for the first step of valine catabolism. Also with the background of the *ILV2 ILV3 ILV5* overexpression, overexpression of *ILV6*, encoding a regulatory subunit that combines with Ilv2, which catalyzes the first committed step in valine biosynthesis, resulted in a three times drop of the yield of isobutanol. We interpret this to be due to an increased sensitivity of Ilv2 to valine inhibition, weakening the positive impact of overexpression of *ILV2*, *ILV3*, and *ILV5* on increasing isobutanol production.

Aerobic cultivation of the *ILV2 ILV3 ILV5* overexpression strain and the reference strain in shake flasks indicated that uptake of valine has the same effect on increasing the valine pool and thereby isobutanol production as on increasing the flux capacity from pyruvate to 2-keto isovalerate by overexpression of the three genes. Thus, the enzyme activities for the supply of 2-keto isovalerate were not a bottleneck any longer in the *ILV2 ILV3 ILV5* overexpression strain. Other bottlenecks, such as the regulation of valine production, export of valine or 2-keto isovalerate from mitochondria to cytosol, or the affinities of PDCs to 2-ketoisovalerate in cytosol, should be investigated in order to further increase the yield of isobutanol.

4.4. Methods

4.4.1. Media and culture conditions

The mineral medium, which was used in all anaerobic fermentations, had the following composition (per liter): $(NH_4)_2SO_4$, 10 g; KH_2PO_4, 6 g; $MgSO_4 \cdot 7H_2O$, 1 g; Antifoam 289 (A-5551; Sigma-Aldrich), 0.2 ml; trace metal solution, 2 ml; vitamin solution, 2 ml; and ergosterol solution, 2 ml. This medium was supplemented with 40 g/liter glucose and 0.1 g/liter uracil. The trace metal solution consisted of the

following (per liter): EDTA (sodium salt), 15.0 g; $ZnSO_4 \cdot 7H_2O$, 4.5 g; $MnCl_2 \cdot 2H_2O$, 0.84 g; $CoCl_2 \cdot 6H_2O$, 0.3 g; $CuSO_4 \cdot 5H_2O$, 0.3 g; $Na_2MoO_4 \cdot 2H_2O$, 0.4 g; $CaCl_2 \cdot 2H_2O$, 4.5 g; $FeSO_4 \cdot 7H_2O$, 3 g; H_3BO_3, 1 g; and KI, 0.1 g. The vitamin solution contained the following (per liter): biotin, 0.05 g; *p*-aminobenzoic acid, 0.2 g; nicotinic acid, 1 g; calcium pantothenate, 1 g; pyridoxine-HCl, 1 g; thiamine-HCl, 1 g; and *myo*-inositol, 25 g. The ergosterol solution contained 2 g ergosterol and 84 g Tween 80 in 100 ml pure ethanol.

For the pre-cultivations, 50 ml of mineral medium was used in 500 ml shake flasks, with the exception that 0.1 g/liter uracil was added when necessary, and no ergosterol was used. The pre-cultures were grown at 30°C with shaking at 200 rpm and a start pH of 5.0.

All aerobic cultivations were performed in 500 ml baffled shake flasks with 100 ml of working volume of either buffered mineral medium or YPD complex medium. Buffered mineral medium contained (per liter): $(NH_4)_2SO_4$, 15 g; KH_2PO_4, 28.8 g; $MgSO_4 \cdot 7H_2O$, 1 g; Antifoam 289, 0.2 ml; trace metal solution, 4 ml; vitamin solution, 2 ml and 40 g glucose. The compositions of trace metal and vitamin solutions were as above. 0.1 g/liter uracil was used when necessary. The YPD complex medium contained, per liter, 10 g of yeast extract, 20 g of peptone, and 17 g glucose. The aerobic cultivations were carried out at 30 °C with shaking at 200 rpm and a start pH of 5.0.

4.4.2. Strains and strain construction

All *S. cerevisiae* strains used in this study were derivatives of CEN.PK 2-1C strain (*MATα leu2-3, 112 his3-Δ1 ura3-52 trp1-289 MAL2-8*(Con) *MAL3 SUC3*) (Table 4.3). Strain CEN.PK 113-5D (*MATα SUC2 MAL2-8*^{c} *ura3-52*) and CEN.PK 113-7D (*MATα MAL2-8*^{c} *SUC2*), were used as reference strains in fermentation and real-time PCR experiments, respectively. For routine cultivation, YPD solid or liquid medium was used. Synthetic drop-out (SD) solid media appropriately lacking uracil or amino acids were used for selection of yeast plasmid transformants. YPG glycerol-based solid medium (containing, per liter, 10 g of yeast extract, 20 g of peptone, and 20 g of

glycerol) was used for petite test before long-term storage of strains in 20% of glycerol at -80°C.

Throughout strain construction, standard molecular biology methods were used. Primers used for PCR amplification of DNA fragments (*PGK1* promoter, genes *ILV2*, *ILV3*, *ILV5*, *ILV6* and *BAT2*) from *S. cerevisiae* are listed in Table 4.4. Each amplified target gene (*ILV2*, *ILV3*, *ILV5*, *ILV6*, or *BAT2*) was fused to the downstream end of the *PGK1* promoter sequence (1480 bp) in subsequent PCR through designed overlapping ends between the promoter and the target gene. All preparative PCRs were performed with Phusion high-fidelity DNA polymerase (Finnzymes).

The generated blunt end fusion PCR products, PGK1+ILV2, PGK1+ILV3, PGK1+ILV5, PGK1+ILV6 or PGK1+BAT2, were cloned into the pCR-Blunt II-TOPO vector by using the Zero Blunt TOPO PCR Cloning Kit (Invitrogen). The resulting plasmids were designated pTOPO_P+ILV2, pTOPO_P+ILV3, pTOPO_P+ILV5, pTOPO_P+ILV6, and pTOPO_P+BAT2, respectively. The *PGK1* promoter together with the target gene were cut out from these pTOPO clones, and ligated into vector YDp-L, YDp-W, YDp-H, YDp-U, and YDp-U [13], respectively. The resulting plamids were designated YDp-L_P+ILV2, YDp-W_P+ILV3, YDp-H_P+ILV5, YDp-U_P+ILV6, and YDp-U_P+BAT2, respectively (Table 4.3). They were digested with *Bgl*II, *Bgl*II, *Eco*RI, *Nar*I, and *Eag*I in the middle of gene *ILV2*, *ILV3*, *ILV5*, *ILV6*, and *BAT2*, respectively. The linearized plasmids were chromosomally integrated into yeast strain CEN.PK 2-1C (a kind gift of Peter Kötter, Frankfurt, Germany) in various combinations. The strain with plasmids YDp-L_P+ILV2, YDp-W_P+ILV3 and YDp-H_P+ILV5 integrated in the genome was designated ILV235_XCY561. The strain with plasmids YDp-L_P+ILV2, YDp-W_P+ILV3, YDp-H_P+ILV5, and YDp-U_P+ILV6 was designated ILV2356_XCY605. Two identical strains, independently isolated in the last step of construction, with plasmids YDp-L_P+ILV2, YDp-W_P+ILV3, YDp-H_P+ILV5, and YDp-U_P+BAT2 were designated ILV235BAT2_XCY715 and ILV235BAT2_XCY723, respectively. The genomic integration of the plasmid was confirmed by PCR amplifying PGK1+ILV2, PGK1+ILV3, PGK1+ILV5,

PGK1+ILV6 or PGK1+BAT2 fragment from the genomic DNA of the constructed overexpression strains.

Table 4.3. Plasmids and strains

Plasmid or strain	Relevant characteristics	Source or reference
Plasmid		
pCR-Blunt II-TOPO	Cloning vector; Km^r	Invitrogen
YDp-L	pUC9 derivative, with *LEU2* marker	[11]
YDp-W	pUC9 derivative, with *TRP1* marker	[11]
YDp-H	pUC9 derivative, with *HIS3* marker	[11]
YDp-U	pUC9 derivative, with *URA3* marker	[11]
pTOPO_P+ILV2	pCR-Blunt II-TOPO with *PGK1* promoter and *ILV2* gene from *S. cerevisiae*	This study
pTOPO_P+ILV3	pCR-Blunt II-TOPO with *PGK1* promoter and *ILV3* gene from *S. cerevisiae*	This study
pTOPO_P+ILV5	pCR-Blunt II-TOPO with *PGK1* promoter and *ILV5* gene from *S. cerevisiae*	This study
pTOPO_P+ILV6	pCR-Blunt II-TOPO with *PGK1* promoter and *ILV6* gene from *S. cerevisiae*	This study
pTOPO_P+BAT2	pCR-Blunt II-TOPO with *PGK1* promoter and *BAT2* gene from *S. cerevisiae*	This study
YDp-L_P+ILV2	Plasmid YDp-L with *PGK1* promoter and *ILV2*	This study
YDp-W_P+ILV3	Plasmid YDp-W with *PGK1* promoter and *ILV3*	This study
YDp-H_P+ILV5	Plasmid YDp-H with *PGK1* promoter and *ILV5*	This study
YDp-U_P+ILV6	Plasmid YDp-U with *PGK1* promoter and *ILV6*	This study
YDp-U_P+BAT2	Plasmid YDp-U with *PGK1* promoter and *BAT2*	This study
Strains		
CEN.PK 2-1C	*MATα leu2-3, 112 his3-Δ1 ura3-52 trp1-289 MAL2-8*(Con) *MAL3 SUC3*	P. Kötter
CEN.PK 113-5D	*MATα SUC2 MAL8^c ura3-52*	P. Kötter
CEN.PK 113-7D	*MATα MAL2-8^c SUC2*	P. Kötter
ILV235_XCY561	CEN.PK 2-1C with YDp-H_P+ILV5, YDp-L_P+ILV2, and YDp-W_P+ILV3 inserted into the genome.	This study
ILV235BAT2_XCY715, ILV235BAT2_XCY723	CEN.PK 2-1C with YDp-H_P+ILV5, YDp-L_P+ILV2, YDp-W_P+ILV3, and YDp-U_P+BAT2 inserted into the genome.	This study
ILV2356_XCY605	CEN.PK 2-1C with YDp-H_P+ILV5, YDp-L_P+ILV2, YDp-W_P+ILV3, and YDp-U_P+ILV6 inserted into the genome.	This study

Table 4.4. Primer sequences

Fragment	Primer	Primer sequence (5' → 3')	Restriction site
PGK1 promoter	Forward	AAAAAACCCGGGTCTAACTGATCTATCCAAAACTG	*Xma*I
	Reverse	TGTTTTATATTTGTTGTAAAAAGTAGA	
ILV2	Forward	TCTACTTTTTACAACAAATATAAAACAATGATCAGACAATCTACGCTAA	
	Reverse	AAAAAAGGCGCCCAAGCTTGCAATTTTTGACG	*Nar*I
ILV3	Forward	TCTACTTTTTACAACAAATATAAAACAATGGGCTTGTTAACGAAAGT	
	Reverse	AAAAAAGGCGCCCTTTGGTAGAGGTGGCTTCG	*Nar*I
ILV5	Forward	TCTACTTTTTACAACAAATATAAAACAATGTTGAGAACTCAAGCCGC	
	Reverse	AAAAAAGGCGCCATTCGCGTTTCGGTTCTTGT	*Nar*I
ILV6	Forward	TCTACTTTTTACAACAAATATAAAACAATGCTGAGATCGTTATTGCA	
	Reverse	AAAAAAGAC GTCAACATCCCAATATCCGTCCA	*Aat*II
BAT2	Forward	TCTACTTTTTACAACAAATATAAAACAATGACCTTGGCACCCCTAGA	
	Reverse	AAAAAAGGCGCC GAATTGTCTTGAGTTGCTTCTAAGGTA	*Nar*I
q*ILV2*	Forward	TCCAAGGTTGCCAACGACACAG	
	Reverse	TGTTGAGCAGCCCACATTTGATG	
q*ILV3*	Forward	TTGCACCTCCACCTCGTTACAC	
	Reverse	ACCGTTGGAAGCGTTGGAAACC	
q*ILV5*	Forward	TTACGCCGTCTGGAACGATGTC	
	Reverse	GAACCAATGGCAACGGCCAAAG	
q*ILV6*	Forward	TACCATGGTGCGTTGCAGTTCC	
	Reverse	AGGTCTTGTTGCGTGTCTGTGC	
q*BAT2*	Forward	GAAATCGGCTGGAAAGGCGAAC	
	Reverse	CTTTGGCCAATGGACCGGTTTG	
q*ACT1*	Forward	TGGATTCTGAGGTTGCTGCTTTGG	
	Reverse	ACCTTGGTGTCTTGGTCTACCG	

[a] Restriction sites used for cloning are underlined. The reverse and complementary sequences used for fusion PCRs are double underlined. The primers for q*ILV2* q*ILV3* q*ILV5* q*ILV6* q*BAT2* and q*ACT1* amplifications were used for quantitative real-time PCRs.

4.4.3. Quantitative real-time PCR

Quantitative real-time PCR was used for quantifying the copy number of the integrated gene and its transcriptional level in the overexpression strain.

Total genomic DNA isolation. The overexpression strains and the reference strain were cultivated with shaking in 10 ml YPD medium at 30 ºC overnight. The cells were harvested and lysed with 0.5 mm acid-washed glass beads in 200 ul of breaking buffer through 3 min of vortexing. The breaking buffer contained 2% Triton X-100,

1% SDS, 100 mM NaCl, 100 mM Tris-Cl and 1 mM EDTA with pH at 8.0. 200 ul 1x TE buffer, which contained 10 mM Tris-HCl and 1 mM EDTA, was added to the lysed cells. After centrifugation at 12000 g for 5 min, the supernatant was transferred into a new Eppendorf tube. The DNA in the supernatant was precipitated with 1 ml of 100% ethanol, washed with 1ml of 70% ethanol twice, and resuspended in 50ul sterile Milli-Q water. The quality and quantity of the isolated genomic DNA was measured using NanoDrop ND-1000 (Thermo Scientific). The isolated gDNA with good purity and appropriate quantity was used as template for quantitative real-time PCR to determine the copy number of the integrated genes in the overexpression strains.

Total RNA isolation. The overexpression strains and the reference stain were cultivated aerobically in mineral medium in shake flasks. Cells were harvested when the optical density of the culture was between 4 and 6 at 600 nm. Total RNA was isolated using TRI REAGENT ^{TM}LS from Sigma as recommended by the manufacturer. The quality and quantity of the isolated RNA was measured using NanoDrop ND-1000. Then DNase treatment was performed to the RNA samples by using DEOXYRIBONUCLEASE I from Sigma. The cDNA was made using M-MuLV RNase H^+ reverse transcriptase and random hexamer primer set provided by DyNAmoTM SYBR Green 2-Step qRT-PCR Kit from FINNZYMES. The negative control of reverse transcription was carried with the RNA which was not treated by DNaseout. The cDNA and the negative controls were used as the template for quantitative real-time PCR to determine the transcriptional level of the target genes in the overexpression strains and the reference strain.

The primers used for amplifying the small parts of *ILV2*, *ILV3*, *ILV5*, *ILV6*, *BAT2*, and the reference gene *ACT1*, are listed in Table 4.3. The resulting PCR fragments' sizes were 80, 74, 72, 76, 73, and 125 bp, respectively. The program used for quantitative PCR reactions was as follows: initial denaturation at 95°C for 15 min; 40 cycles of denaturation at 94°C for 10 s, annealing at 66°C for 30 s, fluorescence data collection, extension at 72°C for 30 s; final extension at 72°C for 10 min; melting curve from 65 to 95°C. The threshold cycles (C(t)s) were calculated with the set threshold value by using Mx3005P software. The delta delta C(t) method was applied for the relative quantification of the copy numbers and the transcription of *ILV2*, *ILV3*,

ILV5, *ILV6*, and *BAT2* in the overexpression strains with respect to the reference strain.

4.4.4. Fermentation

All anaerobic batch fermentations were performed in triplicate in 2-liter fermenters (Braun-Biostat B2, stirred tank) with a working volume of 1.5 liter. The fermenter was inoculated with a pre-culture from a shake flask to an optical density of 0.05 at 600 nm. During cultivation the temperature was maintained at 30°C, agitation was set at 200 rpm, and sparging was kept at 1 liter of pure nitrogen per min. pH was maintained at 5.0 by automatic addition of 2 N NaOH. The CO_2 and O_2 concentrations in the effluent gas from the fermenter were analyzed by gas monitor (Innova 1311). Samples were taken throughout the cultivation for optical density measurement, biomass dry weight determination, and high-performance liquid chromatography analysis. Samples for GC analysis were taken when glucose was depleted (defined by the zero value of CO_2 in the effluent gas).

4.4.5. Analytical methods

Optical density was measured at 600 nm with a Shimadzu UV-Mini 1240 spectrophotometer. Dry weight of biomass was determined gravimetrically by filtration of a known volume of culture over a pre-dried and weighed 0.45 μm-pore-size filter. The filter with biomass was rinsed with a two-fold volume of 0.9% NaCl, dried in a microwave oven at 150 W for 20 min and weighed again.

The concentrations of glucose, pyruvate, acetate, succinate, glycerol, and ethanol were measured by using isocratic high-performance liquid chromatography with refractive Index detection on an Agilent 1100 system (Waldbronn, Germany) equipped with cooled autosampler (5 °C). Separation was conducted on an Aminex HPX-87H ion-exclusion column, and 5 mM of H_2SO_4 as the mobile phase at a flow rate of 0.6 milliliter per minute at 60 °C was used. Twenty μl of sample were injected, and concentrations were determined against freshly prepared external standards.

Isobutanol was determined using static head space-gas chromatography on a PerkinElmer HS 40 Head-space sampler (Waltham, Massachusetts, USA) connected to a Perkin Elmer PE Autosystem gas chromatograph equipped with a Flame Ionization Detector (FID) and 60 m, 0.25 mm ID, 1 µm, DB-5 capillary column. Samples (1 ml in 20 ml sealed head space vials) were equilibrated for 5 min at 60 °C in the auto sampler. The temperature of the needle and the transfer line was 90 °C. Helium carrier gas was used at 20 psi. The temperatures of the injector and the detector were set to 200 °C and 250 °C, respectively. The oven temperature program was 1 min at 60 °C and then 10 °C per min to 150 °C.

Quantification had to be done using standard addition, since the slope of the calibration curve in pure water was different from the one obtained by spiking the fermentation sample with standards. Standard addition was done at three different levels using 50 µl isobutanol standard solutions to certain volume of sample solutions. The corresponding addition were 7-100%, 40-150%, and 57-300% extra isobutanol. R^2 of the corresponding addition curves were in all cases larger than 0.96, and in most cases over 0.98. The initial isobutanol concentration was extrapolated by the readings changed before and after adding the standard solutions. Quantification of 2-methyl butanol and 3-methyl butanol was done by using isobutanol as the internal standard. The response factor differences of 2-methyl butanol and 3-methyl butanol versus isobutanol were determined by calibration with mixtures of isobutanol, 2-methyl butanol and 3-methyl butanol spiked into the media blank, at different concentrations similar to the ones observed in real samples.

Acknowledgements

The authors would like to acknowledge Peter Kötter for providing the applied yeast strain CEN.PK 2-1C. Uffe Hasbro Mortensen is acknowledged for his support and valuable comments. Furthermore, we would like to thank Jesper Mogensen and Jette Jepmond Mortensen for expert technical assistance. The authors gratefully acknowledge a contribution to the fellowship for X.C. from the S.C. Van Foundation, Denmark.

References

1. Connor MR, Liao JC: **Microbial production of advanced transportation fuels in non-natural hosts.** *Curr Opin Biotechnol* 2009, **20:**307-315.
2. Cronk TC, Mattick LR, Steinkraus KH, Hackler LR: **Production of higher alcohols during indonesian tape ketan fermentation.** *Appl Environ Microbiol* 1979, **37:**892-896.
3. Giudici P, Romano P, Zambonelli C: **A biometric study of higher alcohol production in Saccharomyces cerevisiae.** *Can J Microbiol* 1990, **36:**61-64.
4. Atsumi S, Hanai T, Liao JC: **Non-fermentative pathways for synthesis of branched-chain higher alcohols as biofuels.** *Nature* 2008, **451:**86-89.
5. Smith KM, Cho KM, Liao JC: **Engineering Corynebacterium glutamicum for isobutanol production.** *Appl Microbiol Biotechnol* 2010, **87:**1045-1055.
6. Hohmann S: **Osmotic adaptation in yeast-control of the yeast osmolyte system.** In *International Review of Cytology*. Edited by Zeuthen T, Stein WD. California: Academic Press; 2002: 149-188. [*Molecular mechanisms of water transport across biological membranes,* vol 215.]
7. Knoshaug EP, Zhang M: **Butanol tolerance in a selection of microorganisms.** *Appl Biochem Biotechnol* 2009, **153:**13-20.
8. Hazelwood LA, Daran JM, van Maris AJ, Pronk JT, Dickinson JR: **The Ehrlich pathway for fusel alcohol production: a century of research on Saccharomyces cerevisiae metabolism.** *Appl Environ Microbiol* 2008, **74:**2259-2266.
9. Dickinson JR, Harrison SJ, Hewlins MJ: **An investigation of the metabolism of valine to isobutyl alcohol in Saccharomyces cerevisiae.** *J Biol Chem* 1998, **273:**25751-25756.
10. Yoshimoto H, Fukushige T, Yonezawa T, Sone H: **Genetic and physiological analysis of branched-chain alcohols and isoamyl acetate production in Saccharomyces cerevisiae.** *Appl Microbiol Biotechnol* 2002, **59:**501-508.
11. Larry Cameron Anthony A, PA (US), Lixuan Lisa Huang H, DE (US), Rick W. Ye H, DE (US): **Production of isobutanol in yeast mitochondria.** Pub. No.: US 20100129886A1. United States. 2010. Patent.
12. Reid M. Renny Feldman HR, CO (US), Uvini Gunavardena I, CA (US), Jun Urano A, CO (US), Peter Meinhold D, CO (US), Aristos A. Aristidou HR, CO

(US), Catherine Asleson Dundon E, CO (US), Christopher Smith E, CO (US): **Yeast organism producing isobutanol at high yield.** Pub. No.: US 20090226991 A1. United States. 2009. Patent.

13. Berben G, Dumont J, Gilliquet V, Bolle PA, Hilger F: **The YDp plasmids: a uniform set of vectors bearing versatile gene disruption cassettes for Saccharomyces cerevisiae.** *Yeast* 1991, **7:**475-477.
14. Ferreira ID, Rosario VE, Cravo PV: **Real-time quantitative PCR with SYBR Green I detection for estimating copy numbers of nine drug resistance candidate genes in Plasmodium falciparum.** *Malar J* 2006, 5:1.
15. Yi CX, Zhang J, Chan KM, Liu XK, Hong Y: **Quantitative real-time PCR assay to detect transgene copy number in cotton (Gossypium hirsutum).** *Anal Biochem* 2008, 375:150-152.
16. Kispal G, Steiner H, Court DA, Rolinski B, Lill R: **Mitochondrial and cytosolic branched-chain amino acid transaminases from yeast, homologs of the myc oncogene-regulated Eca39 protein.** *J Biol Chem* 1996, **271:**24458-24464.
17. Eden A, Simchen G, Benvenisty N: **Two yeast homologs of ECA39, a target for c-Myc regulation, code for cytosolic and mitochondrial branched-chain amino acid aminotransferases.** *J Biol Chem* 1996, **271:**20242-20245.
18. Lilly M, Bauer FF, Styger G, Lambrechts MG, Pretorius IS: **The effect of increased branched-chain amino acid transaminase activity in yeast on the production of higher alcohols and on the flavour profiles of wine and distillates.** *FEMS Yeast Res* 2006, **6:**726-743.
19. Sentheshanuganathan S: **The mechanism of the formation of higher alcohols from amino acids by Saccharomyces cerevisiae.** *Biochem J* 1960, **74:**568-576.
20. Dickinson JR: **Pathways of leucine and valine catabolism in yeast.** *Methods Enzymol* 2000, **324:**80-92.
21. Cullin C, Baudin-Baillieu A, Guillemet E, Ozier-Kalogeropoulos O: **Functional analysis of YCL09C: evidence for a role as the regulatory subunit of acetolactate synthase.** *Yeast* 1996, **12:**1511-1518.

22. Pang SS, Duggleby RG: **Expression, purification, characterization, and reconstitution of the large and small subunits of yeast acetohydroxyacid synthase.** *Biochemistry* 1999, **38:**5222-5231.

Chapter 5. Application of genome-scale model in metabolic engineering of *Saccharomyces cerevisiae* for improvement of isobutanol production

Xiao Chen*, Irina Borodina; Kaisa Karhumaa; Morten Kielland-Brandt;
Mikael Rørdam Andersen

Abstract

Cellular metabolism is a complex system by nature, and should be analyzed as a whole in metabolic engineering. In this study, the genome-scale stoichiometric model of *Saccharomyces cerevisiae* was applied to find genetic manipulation targets for improvement of isobutanol production in *S. cerevisiae* strains. The BioOpt software, which performs flux balance analysis using linear programming, was used for *in silico* cell metabolism simulation. An updated version of *iFF708* was established and designated *iFF708_IDU*. The positive effect of overexpression of *BAT2* on isobutanol production was achieved in this updated version. In this study, the anaerobic fermentation data of four *S. cerevisiae* strains, three overexpression strains and one reference strain, were compared with their corresponding *in silico* simulation data. A fair agreement was obtained between the experimental data and the simulation results, indicating the feasibility of applying genome-scale model in metabolic engineering. Single gene overexpression and deletion were applied to the overexpression strain ILV2356_XCY605 to predict the possible genetic manipulation targets for overexpression and deletion. Genetic modifications and fermentations should be carried out in order to validate the predicted overexpression and deletion targets for further improvement of isobutanol yield in *S. cerevisiae*.

5.1. Introduction

Metabolic engineering is an effective way to improve strains for a desried property. Finding the correct targeted genes is not easy since cellular metabolism is a complex system by nature. Analysis based on small-scale metabolic pathways may often result in unsuccessful or suboptimal modifications (Kim et al. 2008; Nevoigt 2008). Analysis of the whole metabolic network is more appropriate in principle.

Owing to the important role of *S. cerevisiae* both in industry and academic research, extensive fundamental studies have been carried out (Costanzo et al. 2001; DeRisi et al. 1997; Goffeau 1997; Mewes et al. 2002; Uetz et al. 2000). Its complete genome sequence became available in 1996 (Goffeau et al. 1996). Based on all this knowledge of *S. cerevisiae*, the first genome-scale stoichiometric model, *iFF708*, was established by the research groups of Jens Nielsen and Bernhard Ø. Palsson (Forster et al. 2003a). The model has integrated genomic, biochemical, and physiological information of *S. cerevisiae* at different levels (Forster et al. 2003a).

The *iFF708* model contains 708 structural open reading frames (ORFs), 1175 metabolic reactions and 584 metabolites in total. Establishment of this genome-scale model has made it possible to take the interactions of different pathways into consideration. Based on the overall analysis, we can most likely identify the proper target genes for manipulation (Famili et al. 2003; Forster et al. 2003b).

One possible application of the genome-scale model is within the area of biofuels. The transition to biofuels plays an important role in meeting the challenges of energy security and climate change since the feestocks for biofuel production is sustainable. Isobutanol, with higher energy density, lower hygroscopicity and higher octane number compared to ethanol, has received more and more attention as a potential biofuel. Isobutanol is formed from the valine degradation pathway in cytosol in *S. cerevisiae*, while the valine biosynthetic pathway occurs in mitochondria (Dickinson et al. 1998) (Figure 5.1). The obvious strategy is to direct more carbon from pyruvate to valine and further to isobutanol biosynthetic pathways by overexpression of the genes, *ILV2*, *ILV5*, *ILV3*, *BAT1*, and *BAT2* on the pathway from pyruvate to valine and further to isobutanol. Enzyme Ilv2, Ilv5, and Ilv3 catalyze the reactions from

pyruvate to 3-methyl-2-oxobutanoate, which is the one-step precursor of valine and also named as 2-keto-isovalerate. Enzyme Bat1 and Bat2 are both aminotransferases catalyzing the reversible reaction between 3-methyl-2-oxobutanoate and valine. In a previous study (see Chapter 4), directed genetic manipulations of the valine metabolism by overexpression of *ILV2*, *ILV3*, *ILV5*, and *BAT2* in the pathway in the wild type strain were performed to improve isobutanol production yield. Although the isobutanol production yield was improved nine-fold relative to the wild type strain by this overexpression approach under anaerobic fermentation on glucose, the production yield of isobutanol in the overexpression strain was still too low for industrial application. In order to further increase the isobutanol production yield in *S. cerevisiae*, other genetic manipulations should be considered.

In this study, the genome-scale metabolic model *iFF708_IDU* of *S. cerevisiae* was used in searching for new genetic manipulation targets for improvement of isobutanol production. The BioOpt software was used to perform flux balance analysis with linear programming. By specifying a set of metabolic reactions and defining the constraints for the cultivation conditions, the user can calculate all the internal mass balance fluxes depending on the specified objective.

The model was adjusted for isobutanol production study through several modifications, such as addition of a cytosolic isobutanol biosynthetic pathway and substitution of 3-methyl-2-oxobutanoate transport reaction for L-valine transport reaction from mitochondrion to cytosol in the model formulation. The modifications resulted in an increase in isobutanol production on *BAT2* overexpression, and the correct prediction of *BAT2* as a preferred target for overexpression, which was not observed in the original version, *iFF708*. The updated version, *iFF708_IDU,* also showed the basic physiological behavior of *S. cerevisiae in silico* and a fair agreement between the simulation results predicted by the model and the experimental ones obtained in Chapter 4.

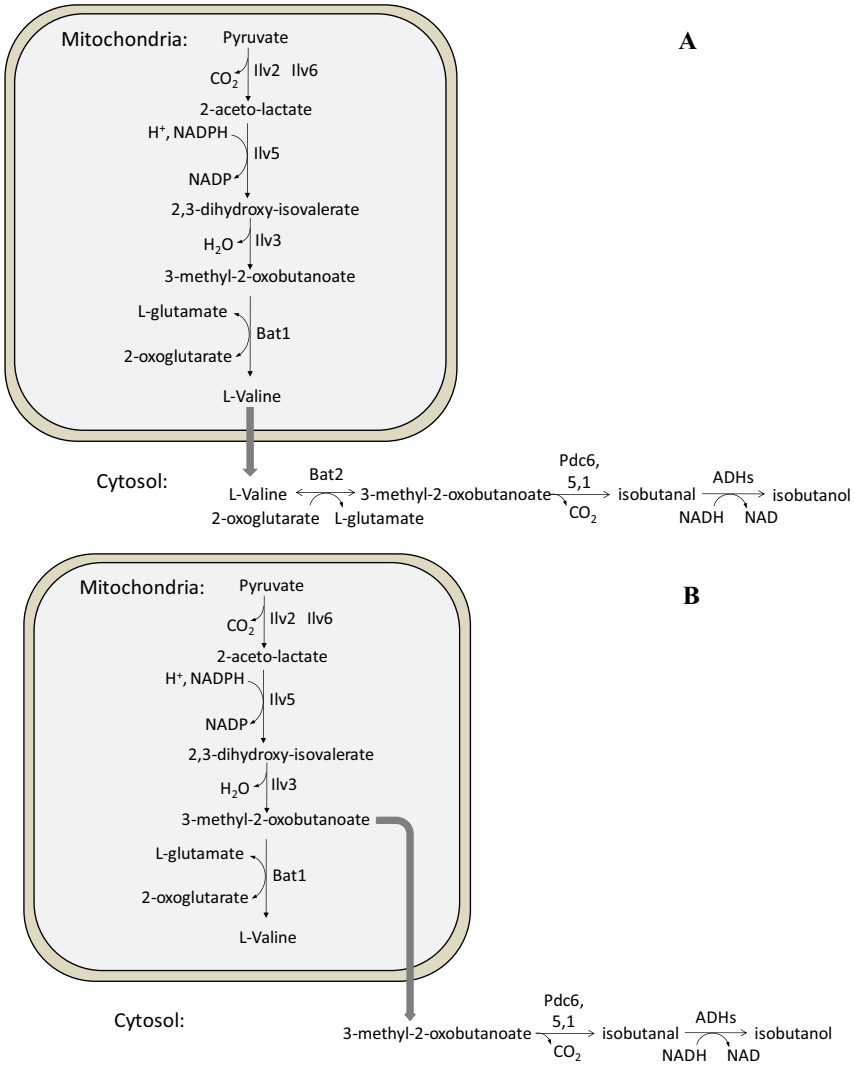

Figure 5.1. A: The isobutanol biosynthetic pathway in *S. cerevisiae* suggested by this study; B: The isobutanol biosynthetic pathway resulting in the addition of the cytosolic steps of Pdc6 and Adh3 to the *iFF708* model.

We also applied the options for prediction of single gene overexpression and deletion by BioOpt to the overexpression strain ILV2356_XCY605 with the anaerobic fermentation on glucose as the reference metabolic state. The genes predicted by the model were *ILV3*, *ILV5*, *ILV2*, *BAT1*, and *BAT2*, which are directly involved in the isobutanol biosynthetic pathway, and *IDP3*, *CTP1*, *PUT2*, *CDC21*, and *CDC8*, which facilitate the formation of NADPH, glutamate, 2-oxoglutarate, and NADH, the

cofactors used in valine and isobutanol biosynthetic pathways. Simulation of single gene deletion showed that deletion of *MDH1, LSC2, KGD1,* or *YAT1,* which are involved in the tricarboxylic acid cycle (TCA cycle), released the pyruvate used for TCA cycle for valine and isobutanol biosynthesis. The simulation data also showed that deletion of gene *GLY1* facilitated the use of a NADH forming reaction for glycine biosynthesis, and thereby facilitated isobutanol production in cytosol. This study proved the prediction capability of the genome-scale model. However, real genetic modifications and fermentations should be carried out to verify these predictions made by the model.

5.2. Methods

5.2.1. Experimental data

The experimental data used in this study are obtained from anaerobic fermentations of *S. cerevisiae* strains (listed in Table 5.1) on glucose in mineral medium at 30 °C.

The detailed description of the plasmids used for the construction of the overexpression strains and the anaerobic fermentations performed are described in the Methods section of Chapter 4.

Table 5.1. Strains, of which the anaerobic fermentation data was used in the study

Strain	Relevant characteristics	Description of the genotype	Source or reference
CEN.PK 113-5D	*MATα SUC2 MAL8^{c} ura3-52*	Wild type	P. Kötter
ILV235_XCY561	CEN.PK 2-1C with YDp-H_P+ILV5, YDp-L_P+ILV2, and YDp-W_P+ILV3 inserted into the genome.	With gene *ILV2 ILV3 ILV5* overespressed	Chapter 4
ILV2356_XCY605	CEN.PK 2-1C with YDp-H_P+ILV5, YDp-L_P+ILV2, YDp-W_P+ILV3, and YDp-U_P+ILV6 inserted into the genome.	With gene *ILV2 ILV3 ILV5 ILV6* overespressed	Chapter 4
ILV235BAT2_XCY715, ILV235BAT2_XCY723	CEN.PK 2-1C with YDp-H_P+ILV5, YDp-L_P+ILV2, YDp-W_P+ILV3, and YDp-U_P+BAT2 inserted into the genome.	With gene *ILV2 ILV3 ILV5 BAT2* overespressed	Chapter 4

5.2.2. Model and simulation tool

All modeling was made based on the *S. cerevisiae iFF708* model (Forster et al. 2003a), or an updated version of it, *iFF708*_IDU, which was established in this study. The BioOpt software, a commercially available linear programming (LP) solver from Lindo Systems Inc, was used as the simulation tool. Simulation calculations were performed using LP with an objective function, which is specific according to individual experiments as described in Forster et al. (2003a).

The compartmentalization of the reactions for the isobutanol biosynthesis in the *iFF708* model did not agree with our hypothesis, in which L-valine is first produced in the mitochondrion, and then exported to the cytosol and degraded into 3-methyl-2-oxobutanoate in the cytosol. The 3-methyl-2-oxobutanoate is converted into isobutanol in two steps. The updated version, *iFF708*_IDU, was made with the following changes in the model formulation relative to *iFF708*: 1) insertion of a cytosolic isobutanol production pathway. Reactions of conversion of 3-methyl-2-oxobutanoate to isobutanol and further to isobutanol, which are catalyzed by *PDC6, PDC5, PDC1, ADH1, ADH2, ADH3, ADH4, ADH5,* and *SFA1,* were added; 2) addition of an extra mitochondrial function of *BAT1* for formation of L-valine from 3-methyl-2-oxobutanoate; 3) substitution of 3-methyl-2-oxobutanoate transport reaction from mitochondrion to cytosol for L-valine transport reaction from mitochondrion to cytosol; 4) since the model prefers to produce L-leucine rather than to produce isobutanol, the export flux of L-leucine from cytosol to the extracellular space was setted to zero in order to study the isobutanol production *in silico*.

5.2.2. General settings for stating different genetic and metabolic backgrounds

The fluxes in both *iFF708* and *iFF708*_IDU model were set to fit the genetic background of the strain and the experimental conditions. The growth mineral medium with uracil supplemented was presented by including the components on a one gram glucose basis as follows: glucose is from 0 to 5.55 mmol; $NH_4^+$is from 0 to 3.8 mmol; PO_4^{3-} is from 0 to 1.1 mmol; SO_4^{2-} is from 0 to 0.1 mmol; uracil is from 0 to 0.022 mmol. If the model simulation led to a flux equal to zero, the flux was reset

to its corresponding experimental value. The overexpression background for *ILV2*, *ILV3*, *ILV5*, and *BAT2* overexpression was modeled by increasing the original flux catalyzed by these genes by 12.5 %. Oxygen uptake was set to zero to simulate the anaerobic condition. The *URA3* gene was deleted in the background if the strain is uracil auxotrophic.

5.2.3. Single gene deletions

Single gene deletion predictions were performed by using the built-in option in BioOpt for single gene deletion. The model was run by setting biomass growth as the objective function. The predicted knockout strains with increased isobutanol yield compared to the overexpression strain ILV2356_XCY605 were examined.

5.2.4. Overexpression studies

The effects of overexpressing single genes on isobutanol yield were studied by applying the built-in option in BioOpt for single gene overexpression. Biomass growth was set as the objective function. The predicted overexpressions with increased isobutanol yield compared to the overexpression strain ILV2356_XCY605 were examined.

5.3. Results and discussions

The genome-scale metabolic stoichiometric model, *iFF708_IDU*, the updated version of *iFF708*, was applied to searching genetic manipulation targets for improvement of isobutanol production in *S. cerevisiae* strain with gene *ILV2*, *ILV3*, *ILV5*, and *BAT2* overexpressed, ILV2356_XCY605.

5.3.1. Verification of the metabolic simulation model

First, the model was checked for its ability of describing the basic physiological characteristics of *S. cerevisiae*. The flux distribution of the wild type under aerobic and anaerobic cultivations on glucose was simulated using biomass yield as the

objective function. The simulation results showed that a large increase in ethanol production was obtained when oxygen uptake rate was set to zero in the model, and under aerobic fermentation conditions high CO_2 and low ethanol productions were observed. The simulation results are in agreement with the physiological characteristics of *S. cerevisiae*.

The cytosolic isobutanol biosynthetic pathway, or in other words the cytosolic valine degradation pathway, which are catalyzed by Pdc1, Pdc5, Pdc6, Adh1, Adh2, Adh3, Adh4, Adh5, and Sfa1, together with the reactions, the formation of valine from 3-methyl-2-oxobutanoate and the formation of 3-methyl-2-oxobutanoate from valine catalyzed by Bat1 in mitochondria, were added in the model formulation as described in the Methods section.

The original model *iFF708* with the addition of isobutanol synthesis pathway has a preference to make isobutanol from 3-methyl-2-oxobutanoate, which is transported from mitochondria to cytosol, through the catalyzation of *PDCs* and *ADHs* enzymes in cytosol. However, our hypothesis is that most of isobutanol is made from valine, which is transported from mitochondria, through the three steps catalyzed with the enzymes encoded by *BAT2*, *PDCs*, and *ADHs* in cytosol. Based on this hypothesis, the reaction of transporting 3-methyl-2-oxobutanoate from mitochondrion to cytosol is substituted for reaction of transporting L-valine from mitochondrion to cytosol in the model formulation. The model with the above modifications was designated *iFF708_IDU*.

The prediction capability of this model, *iFF708_IDU*, was checked through comparison of the anaerobic fermentation data for four *S. cerevisiae* strains and the *in silico* simulation data under the same genetic and metabolic background. These four *S. cerevisiae* strains were CEN.PK 113-5D, ILV235_XCY561, ILV2356_XCY605, and ILV235BAT2_XCY715/723. The metabolic background was anaerobic fermentation in mineral medium with glucose as the growth-limiting substrate and with uracil supplemented. The setting of the genetic and metabolic background in the model was done as described in the Methods section. Known experimental fluxes which were predicted to be zero by the model, namely the pyruvate and acetate yields

in all four strains and the isobutanol and glycerol yields in CEN.PK 113-5D, were replaced with the experimental data in the model formulation. With these fixed yields, the yields of other major metabolites, including biomass, ethanol, succinate, CO_2, isobutanol (not in wild type) and glycerol (not in wild type), were predicted again by the model and compared with the experimental data (Table 5.2). It was shown that most of the predicted data were close to the experimental data. This result indicates that the model should have a fair prediction ability with these specific cultivation conditions and the genetic background.

To further validate the pathway changes made to the metabolic model (see Figure 5.1), predictions of the effect of single gene overexpression on isobutanol yield were performed to strain CEN.PK 113-5D with biomass yield as the objective function in model *iFF708* and *iFF708_IDU*. The simulation results showed that the overexpression of gene *BAT2*, which encodes cytoplasmic branched-chain amino acid aminotransferase catalyzing the first step of valine degradation in cytosol, had no effect on isobutanol production according to the predictions of model *iFF708*. However, this result does not agree with our earlier experimental observation that overexpression of *BAT2* enhanced isobutanol production yield by two-fold (Chapter 4). With the modified model, *iFF708_IDU*, increased isobutanol yield on *BAT2* overexpression was achieved *in silico*.

5.3.2. Prediction of further genetic manipulation targets in ILV2356_XCY605

In order to further improve isobutanol production yield in *S. cerevisiae*, a study of the effect of single gene overexpression or deletion on isobutanol production yield was performed in model *iFF708_IDU*. Strain ILV2356_XCY605 was chosen for this analysis due to the accurate predictions of the fluxes in this strain by *iFF708_IDU* in the previous model prediction ability test (Table 5.2). In the formulation of the model, the genetic and metabolic reference state was set as anaerobic fermentation in mineral medium with glucose as the growth-limiting substrate and with the genes *ILV2, ILV3,* and *ILV5* overexpressed. The overexpressions and knockouts, which would be feasible to perform and could give as much as 20% more isobutanol production yield according to the prediction, are discussed in below.

5.3.2.1 Overexpression targets in ILV2356_XCY605

Single gene overexpression prediction was performed with the built-in single gene overexpression option of BioOpt by optimization for growth. The genes, which gave more than 20% increased isobutanol production yield when it was overexpressed in the model, together with the simulated isobutanol production yield and the growth of the strain are listed in Table 5.3. Gene *ILV3*, *ILV5*, *ILV2*, and *ILV6*, which were already overexpressed in ILV2356_XCY605, were suggested to be further overexpressed by the model. Firstly, this is a further confirmation of the validity of the predictions. Secondly, this suggests that stronger overexpression of these genes, like insertion of multiple copies of these genes in *S. cerevisiae* genome, could be applied in the future strain construction. *BAT1*, which catalyzes the bidirectional reaction between 3-methyl-2-oxobutanoate and valine in mitochondria, was also suggested as an overexpression target by the model. Overexpression of *IDP3*, the isocitrate dehydrogenase, and *CTP1*, the mitochondrial inner membrane citrate transporter, resulted in an increase of 2-oxoglutarate formation in the cytosol in the simulation. Since 2-oxoglutarate is the co-factor needed for conversion of valine to 3-methyl-2-oxobutanoate, overexpression of *IDP3* and *CTP1* could have the possibility of facilitating the formation of isobutanol in the cell.

PUT2, encoding the enzyme that is involved in proline degradation pathway in mitochondria, was also predicted as an overexpression target by the model. The reaction catalyzed by *PUT2* encoded enzyme generates NADPH and glutamate as by-products in mitochondria, which are needed for valine biosynthesis from pyruvate. As a result, overexpression of *PUT2* could also probably facilitate the valine biosynthesis in mitochondria, and thereby the isobutanol production in cytosol.

CDC21, encoding the thymidylate synthase, and *CDC8*, encoding the thymidylate and uridylate kinase, which are used in the biosynthesis of pyrimidine deoxyribonucleotides in cytosol, were also in the list of predicted overexpression targets by the model. The analysis of the *S. cerevisiae* metabolic network showed that overexpression of these genes facilitated the use of METTHF, and the METTHF formation process generates NADH. NADH is used in the formation of isobutanol

from isobutanal. In the model simulation, overexpression of *CDC21* and *CDC8* assisted the isobutanol production since more NADH was generated in the cytosol.

In summary, besides the genes directly involved in the isobutanol biosynthetic pathway, *ILV3*, *ILV5*, *ILV2*, *BAT2*, and *BAT1*, the model preferred to generate more glutamate and cofactor NADPH in mitochondria, and 2-oxoglutarate and reaction cofactor NADH in cytosol, which are needed in isobutanol biosynthetic pathway, by overexpressing genes, *IDP3*, *CTP1*, *PUT2*, *CDC21*, and *CDC8* in order to facilitate the isobutanol production.

5.3.2.2 Deletion targets in ILV2356_XCY605

Single gene deletion prediction was performed with the built-in single gene deletion option of BioOpt by optimization for growth. The knockouts, which gave increased isobutanol yield, together with their isobutanol production yield and the growth of the strain (biomass yield) are listed in Table 5.4. The viability of these knockouts was verified by examination of the *Saccharomyces* genome database (http://www.yeastgenome.org).

In Table 5.4, gene *MDH1*, encoding mitochondrial malate dehydrogenase, gene *LSC2*, encoding beta subunit of succinyl-CoA ligase, and gene *KGD1*, encoding component of the mitochondrial alpha-ketoglutarate dehydrogenase complex, are involved in the tricarboxylic acid (TCA) cycle in mitochondria and were all predicted to facilitate isobutanol production with their deletions. Deletion of gene *YAT1* encoding the outer mitochondrial carnitine acetyl transferase, which is involved in transport of activated acyl groups from the cytoplasm to the mitochondrial matrix needed for the TCA cycle, was predicted by the model as well. All these single gene deletions would result in the disruption of the TCA cycle and the decrease of the ATP formation rate in mitochondria in *S. cerevisiae*, even though the cell still stays viable. Since the TCA cycle is competing for pyruvate with the valine biosynthetic pathway in mitochondria (Figure 5.1), the model suggests shuting down the TCA cycle to facilitate valine biosynthesis in mitochondria, and thus isobutanol production in cytosol.

According to the simulation results, deletion of gene *GLY1*, which encodes threonine aldolase that catalyzes the cleavage of L-allo-threonine and L-threonine to glycine, disrupted the formation of glycine and acetaldehyde from threonine, and resulted in use of the reaction: L-threonine + NAD^+ → acetate + glycine + NADH for glycine production. In other words, deletion of *GLY1* resulted in the increase of NADH level in cytosol, and thus assisted the production of isobutanol in the model.

Table 5.2. Comparision of the anaerobic fermentation data of four S. cerevisiae strains with the *in silico* calculated data by *iFF708*_IDU

Yield (mmol/g glucose)		Isobutanol	Biomass[c]	Ethanol	Pyruvate	Succinate	Glycerol	Acetate	CO_2
CEN.PK 113-5D	Experimental data	0.002	0.102	8.204	0.012	0.014	1.088	0.129	7.319
	Modeling data	0.002	0.097	8.303	0.012	0.034	1.088	0.129	8.907
	Deviation		5%	1%		147%			22%
ILV235_XCY561	Experimental data	0.013	0.105	8.092	0.018	0.005	0.942	0.149	8.75
	Modeling data	0.085	0.086	8.303	0.018	0.114	0.79	0.149	8.876
	Deviation	550%	18%	3%		1982%	16%		1%
ILV2356_XCY605	Experimental data	0.005	0.105	7.988	0.031	0.03	1.073	0.117	9.198
	Modeling data	0.009	0.101	8.882	0.031	0.042	0.501	0.117	9.195
	Deviation	92%	4%	11%		43%	53%		0%
ILV235BAT2_XCY715 /723	Experimental data	0.029	0.073	7.32	0.036	0.024	1.027	0.186	8.474
	Modeling data	0.013	0.096	8.776	0.036	0.045	0.461	0.186	9.07
	Deviation	56%	32%	20%		87%	55%		7%

[a]The data in a yellow box were fixed with the experimental data since they were predicted as zero in the simulation.
[b]The data in a green box stands for the predicted data by the model.
[c]The biomass yield is presented as gram biomass per gram glucose.

Table 5.3. The overexpression targets predicted by genome-scale model *iFF708*_IDU

Overexpressed gene	Name	Predicted isobutanol production (mmol/g glc)	Predicted growth (g/g glc)
/	No overexpression	0.0089	0.1010
ILV3	Dihydroxy-acid dehydratase, mitochondrial	0.0286	0.0973
ILV5	Ketol-acid reductoisomerase, mitochondrial	0.0286	0.0973
ILV2	Acetolactate synthase catalytic subunit, mitochondrial	0.0286	0.0973
BAT2	Branched-chain-amino-acid aminotransferase, cytosolic	0.0147	0.1001
BAT1	Branched-chain-amino-acid aminotransferase, mitochondrial	0.0208	0.0991
IDP3	Isocitrate dehydrogenase [NADP]	0.0104	0.0990
CTP1	Tricarboxylate transport protein, exchange of citrate and isocitrate from cytosol to mitochondrion	0.0104	0.0990
PUT2	Delta-1-pyrroline-5-carboxylate dehydrogenase, mitochondrial	0.0348	0.0968
CDC21	Thymidylate synthase	0.0864	0.0795
CDC19	Pyruvate kinase 1	0.0212	0.0847
CDC8	Thymidylate kinase	0.1176	0.0809

Table 5.4. The deletion targets predicted by genome-scale model *iFF708*_IDU

Gene	Name	Predicted isobutanol production (mmol/g glc)	Predicted growth (g/g glc)
/	No deletion	0.0089	0.1010
MDH1	Alpha-ketoglutarate dehydrogenase	0.0194	0.0871
LSC2	Beta subunit of succinyl-CoA ligase	0.0129	0.0957
KGD1	Component of the mitochondrial alpha-ketoglutarate dehydrogenase complex	0.0129	0.0957
YAT1	Putative mitochondrial carnitine O-acetyltransferase	0.0105	0.0988
GLY1	Low specificity L-threonine aldolase	0.0105	0.0989

5.4. Conclusions and future perspectives

In this study, a genome-scale model of *S. cerevisiae* was applied to searching for potential genetic manipulation targets for further improvement of isobutanol production yield in the isobutanol-producing strain ILV2356_XCY605. To adjust the original model *iFF708* for isobutanol production study, several modifications were made, such as integration of a cytosolic isobutanol biosynthetic pathway, and substitution of 3-methyl-2-oxobutanoate transport reaction for L-valine transport reaction from mitochondrion to cytosol in the model formulation. The modified model was designated *iFF708_IDU*. With the modified model, an increase of isobutanol yield was achieved when gene *BAT2*, which encodes the branched-chain amino acid aminotransferase catalyzing the first step of valine degradation in cytosol, was overexpressed in the model. This *in silico* simulation result was consistent with the experimental one carried out in Chapter 4. The fact that the anaerobic fermentation data of four *S. cerevisiae* strains was fairly consistent with their corresponding *in silico* simulation, indicates that the genome-scale model has a reasonable prediction capability under specific genetic and metabolic conditions.

In silico single gene overexpression and deletion analysis were carried out with biomass yield as the objective function in the model *iFF708_IDU* using ILV2356_XCY605 as the reference strain. The simulation results showed that further overexpression genes, *ILV3, ILV5, ILV2, BAT1,* and *BAT2*, which are directly involved in the isobutanol biosynthetic pathway, increased isobutanol production yield. Moreover, overexpression of genes, *IDP3, CTP1, PUT2, CDC21,* and *CDC8*, resulted in formation of more NADPH and glutamate in the mitochondria, and more 2-oxoglutarate and NADH in the cytosol, which are the cofactors used in valine and isobutanol biosynthetic pathways. Increase of these cofactors facilitated the isobutanol production. Simulation of single gene deletion showed that deletion of *MDH1, LSC2, KGD1,* or *YAT1,* which are involved in the TCA cycle, disrupted the TCA cycle in mitochondria, and released the pyruvate used for TCA cycle for valine biosynthesis, and further enhanced the isobutanol biosynthesis. Deletion of gene *GLY1* facilitated the use of a NADH forming reaction for glycine biosynthesis, and thereby facilitated isobutanol production in cytosol.

All these *in silico* improvements of isobutanol production yield caused by the above genetic manipulations suggested by the model should be verified through real experiments in the future.

References

Costanzo MC, Crawford ME, Hirschman JE, Kranz JE, Olsen P, Robertson LS, Skrzypek MS, Braun BR, Hopkins KL, Kondu P and others. 2001. YPD, PombePD and WormPD: model organism volumes of the BioKnowledge library, an integrated resource for protein information. Nucleic Acids Res 29(1):75-9.

DeRisi JL, Iyer VR, Brown PO. 1997. Exploring the metabolic and genetic control of gene expression on a genomic scale. Science 278(5338):680-6.

Dickinson JR, Harrison SJ, Hewlins MJ. 1998. An investigation of the metabolism of valine to isobutyl alcohol in Saccharomyces cerevisiae. J Biol Chem 273(40):25751-6.

Famili I, Forster J, Nielsen J, Palsson BO. 2003. Saccharomyces cerevisiae phenotypes can be predicted by using constraint-based analysis of a genome-scale reconstructed metabolic network. Proc Natl Acad Sci U S A 100(23):13134-9.

Forster J, Famili I, Fu P, Palsson BO, Nielsen J. 2003a. Genome-scale reconstruction of the Saccharomyces cerevisiae metabolic network. Genome Res 13(2):244-53.

Forster J, Famili I, Palsson BO, Nielsen J. 2003b. Large-scale evaluation of in silico gene deletions in Saccharomyces cerevisiae. OMICS 7(2):193-202.

Goffeau A. 1997. The yeast genome directory. Nature 387(6632 Suppl):5.

Kim TY, Sohn SB, Kim HU, Lee SY. 2008. Strategies for systems-level metabolic engineering. Biotechnol J 3(5):612-23.

Mewes HW, Frishman D, Guldener U, Mannhaupt G, Mayer K, Mokrejs M, Morgenstern B, Munsterkotter M, Rudd S, Weil B. 2002. MIPS: a database for genomes and protein sequences. Nucleic Acids Res 30(1):31-4.

Nevoigt E. 2008. Progress in metabolic engineering of Saccharomyces cerevisiae. Microbiol Mol Biol Rev 72(3):379-412.

Uetz P, Giot L, Cagney G, Mansfield TA, Judson RS, Knight JR, Lockshon D, Narayan V, Srinivasan M, Pochart P and others. 2000. A comprehensive analysis of protein-protein interactions in Saccharomyces cerevisiae. Nature 403(6770):623-7.

Chapter 6. Conclusions and future perspectives

This thesis represents an effort for further developing *S. cerevisiae* as a cell factory for production of two chemicals of industrial interest: δ-(L-α-aminoadipyl)–L-cysteinyl–D-valine (LLD-ACV) as a nonribosomal peptide and isobutanol as biofuel. Production of both chemicals was realized by metabolic engineering of the amino acid metabolism in *S. cerevisiase*, which was chosen due to its several favourable traits for a large scale industrial fermentation.

Conclusions regarding production of LLD-ACV

The *Penicillium chrysogenum* gene *pcbAB* encoding ACV synthetase was expressed in *S. cerevisiae* from a high-copy plasmid together with phosphopantetheinyl transferase (PPTase) encoding genes from *Aspergillus nidulans*, *P. chrysogenum* and *Bacillus subtilis*, and in all the three cases production of ACV was observed.

Several factors were investigated to improve ACV synthesis. Codon optimization of 5' end of *pcbAB* did not significantly increase ACV production. However, a 30-fold enhancement was achieved by lowering the cultivation temperature from 30 to 20 ºC.

When ACVS and PPTase encoding genes were integrated into the yeast genome a 6-fold decrease in ACV production was observed, indicating that gene copy number was one of the rate-limiting factors for ACV production in yeast.

Conclusions regarding production of isobutanol

By simultaneous overexpression of genes *ILV2*, *ILV3*, and *ILV5* in valine metabolism pathway in anaerobic fermentation of glucose in mineral medium in *S. cerevisiae*, the isobutanol yield was improved from 0.16 to 0.97 mg per g glucouse. The yield was further improved by two times by the additional expression of *BAT2*, encoding the cytoplasmic branched-chain amino acid aminotransferase. However, overexpression of *ILV6*, encoding the regulatory subunit of Ilv2, in the *ILV2 ILV3 ILV5* overexpression strain decreased the yield by three times, presumably by increasing the

sensitivity of Ilv2 to valine inhibition, thus weakening the positive impact of overexpression of *ILV2*, *ILV3*, and *ILV5* on isobutanol production.

Aerobic cultivations of the *ILV2 ILV3 ILV5* overexpression strain and the reference strain showed that the supply of amino acids in cultivation media gave a substantial improvement in isobutanol yield for the reference strain, but not for the *ILV2 ILV3 ILV5* overexpression strain, which implies that other constraints besides the enzyme activities for the supply of 2-ketoisovalerate may become bottlenecks for isobutanol production after *ILV2*, *ILV3*, and *ILV5* have been overexpressed, and it most probably includes the valine inhibition to Ilv2.

For further improvement of isobutanol production yield in the isobutanol-producing strain ILV2356_XCY605, a genome-scale model of *S. cerevisiae* was applied to searching for potential genetic manipulation targets. Several modifications were made to adjust the original model *iFF708* for isobutanol production study. The resulting model *iFF708_IDU* was used for *in silico* simulation and the results were in fair agreement with the experimental data. Analysis of single gene overexpression and deletion was then carried out with biomass yield as the objective function in the model *iFF708_IDU*. A number of genes to be overexpressed or deleted were suggested while the predictions are subject to further verification by genetic modification and fermentation study.

Future perspectives

Supply of L-α-aminoadipyl in *S. cerevisiae* could be a bottleneck in ACV production. Increasing L-α-aminoadipyl biosynthesis in *S. cerevisiae* through metabolic engineering of its biosynthetic pathway should be considered for further improvement of ACV production.

The regulation of Ilv6 for valine biosynthesis may be a limiting factor for increasing valine production in mitochondria, which can restrict the further improvement of isobutanol production in cytosol. One possible solution is to move the pathway from pyruvate to 2-keto-isovalerate from mitochondria to cytosol. The genome-scale model should be modified accordingly and then used to predict genetic manipulation targets.

CMB is an Engineering Center of Excellence funded by the Danish Research Agency. It is a collaboration between an acknowledged research manager, his/her institute and university, and the Research Agency. An Engineering Center of Excellence is a research institute of first-class quality with tradition for cooperation with industry.

Center for Microbial Biotechnology
Department of Systems Biology
Technical University of Denmark

Building 223
DK-2800 Kgs. Lyngby
Denmark

Phone: +45 4525 26900
Fax: +45 4588 4148

www.cmb.dtu.dk

ISBN-nr: 9788791494994